WL-TR-93-2049

TWO-DIMENSIONAL, HIGH FLOW, PRECISELY CONTROLLED MONODISPERSE DROP SOURCE

JOHN L. DRESSLER

FLUID JET ASSOCIATES
1216 WATERWYCK TRAIL
SPRING VALLEY OH 45370

MAR 1993

FINAL REPORT FOR 11/08/89-03/08/93

AERO PROPULSION AND POWER DIRECTORATE
WRIGHT LABORATORY
AIR FORCE MATERIEL COMMAND
WRIGHT-PATTERSON AFB OH 45433-7650

NOTICE

When Government drawings, specifications, or other data are used for any purpose other than in connection with a definitely Government-related procurement, the United States Government incurs no responsibility for any obligation whatsoever. The fact that the Government may have formulated or in any way supplied the said drawings, specifications, or other data, is not to be regarded by implication, or otherwise in any manner construed, as licensing the holder, or any other person or corporation; or as conveying any rights or permission to manufacture, use, or sell any patented invention that may in any way be related thereto.

This report is releasable to the National Technical Information Service (NTIS). At NTIS, it will be available to the general public, including foreign nations.

This technical report has been reviewed and is approved for publication.

ROBERT D. HANCOCK, Capt, USAF
Fuels Branch
Fuels & Lubrication Division
Aero Propulsion & Power Directorate

ROYCE P. BRADLEY
Section Chief, Fuels Branch
Fuels & Lubrication Division
Aero Propulsion & Power Directorate

LEO S. HAROOTYAN, JR., Chief
Fuels & Lubrication Division
Aero Propulsion & Power Directorate

If your address has changed, if you wish to be removed from our mailing list, or if the addressee is no longer employed by your organization, please notify WL/POSF, WPAFB OH 45433-7103 to help us maintain a current mailing list.

Copies of this report should not be returned unless return is required by security considerations, contractual obligations, or notice on a specific document.

DISCLAIMER NOTICE

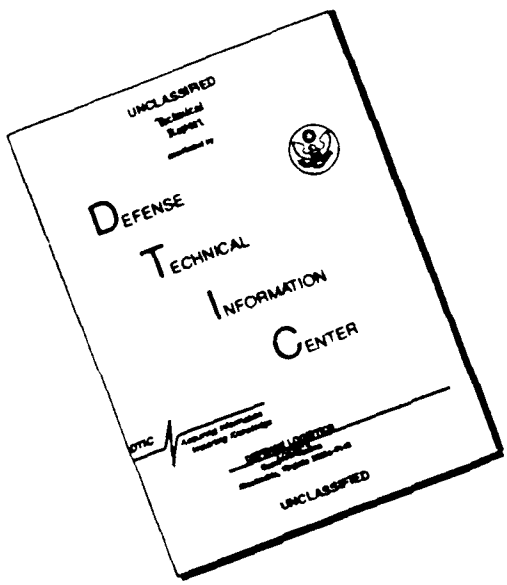

THIS DOCUMENT IS BEST QUALITY AVAILABLE. THE COPY FURNISHED TO DTIC CONTAINED A SIGNIFICANT NUMBER OF PAGES WHICH DO NOT REPRODUCE LEGIBLY.

REPORT DOCUMENTATION PAGE

Form Approved
OMB No. 0704-0188

1. AGENCY USE ONLY (Leave blank)	2. REPORT DATE	3. REPORT TYPE AND DATES COVERED
	15 March 1993	Final - 8 Nov 89-8 Mar 93

4. TITLE AND SUBTITLE
Two-Dimensional, High Flow, Precisely Controlled Monodisperse Drop Source

5. FUNDING NUMBERS
C - F33615-89-C-2973
PE - 65502
PR - 3005
TA - 21
WU - 65

6. AUTHOR(S)
Dr. John L. Dressler

7. PERFORMING ORGANIZATION NAME(S) AND ADDRESS(ES)
Fluid Jet Associates
1216 Waterwyck Trail
Spring Valley OH 45370

8. PERFORMING ORGANIZATION REPORT NUMBER
NA

9. SPONSORING/MONITORING AGENCY NAME(S) AND ADDRESS(ES)
Aero Propulsion and Power Directorate
Wright Laboratory
Air Force Materiel Command
Wright-Patterson AFB OH 45433-7650

10. SPONSORING/MONITORING AGENCY REPORT NUMBER
WL-TR-93-2049

11. SUPPLEMENTARY NOTES
This is a Small Business Innovative Research Program, Phase II

12a. DISTRIBUTION/AVAILABILITY STATEMENT
Approved for public release; distribution is unlimited

12b. DISTRIBUTION CODE

13. ABSTRACT (Maximum 200 words)

A versatile acoustically-driven fluid atomizer was designed and operated that creates precise monodisperse sprays by Rayleigh breakup or polydisperse sprays by the acoustic driving of amplitude dependent instabilities. The atomizer forms a cylindrical, conical, or flat (sheet) liquid jet by means of a photofabricated nozzle. The spray pattern and spray volume are altered by changing the nozzle. A piezoelectric driver, constructed to efficiently couple energy to the liquid, modulates the fluid velocity. When operated at low power, the drop generator can produce arrays of monodisperse drops as small as 15 microns in diameter. Operating the piezoelectric driver at high power produces perturbations with sufficient energy to break the liquid jets into drops, with a net increase in surface energy. The resulting drop sizes are influenced by the frequency and amplitude of the driving signal and nozzle size. The spatial distribution of the spray is controlled by the spacing and geometry of the holes in the nozzle plate, the amplitude of the acoustic signal, and the swirl in the fluid manifold. This device is more robust than the typical acoustic drop generator because small drops can be made from large holes, reducing the plugging problem. No air flow is used.

14. SUBJECT TERMS
Droplet, Sprays, Monodisperse, Polydisperse, Acoustically-driven, Spray Generator, Nozzle, Droplet Generator

15. NUMBER OF PAGES
64

16. PRICE CODE

17. SECURITY CLASSIFICATION OF REPORT	18. SECURITY CLASSIFICATION OF THIS PAGE	19. SECURITY CLASSIFICATION OF ABSTRACT	20. LIMITATION OF ABSTRACT
UNCLASSIFIED	UNCLASSIFIED	UNCLASSIFIED	UL

Contents

List of Figures

1 Introduction

In Phase I of this contract, the atomization of fluids by two different acoustic mechanisms was demonstrated. The creation of novel nozzle geometries by photofabrication was also demonstrated. The purpose of this contract is to develop commercially important sprayers based on the acoustic atomization techniques and nozzle fabrication methods that were demonstrated in Phase I.

Two distinct mechanisms for acoustic drop production were identified in Phase I. The first mechanism is the establishment of initial conditions for the existing varicose instability on a cylindrical jet, commonly called Rayleigh breakup. Rayleigh breakup is driven by surface tension and requires only a low level of acoustic excitation to atomize the cylindrical jet into a monodisperse spray.

The second mechanism is the driving of higher-order modes of instability on fluid sheets and cylinders. In the second case, the modes are normally stable due to surface tension forces and they depend on the energy in the acoustic drive to grow large enough to form a spray. If the acoustic signal is removed, the atomization ceases. Since these modes of fluid deformation require a drive of sufficient amplitude to overcome surface tension and form a spray, we call them amplitude-dependent instabilities.

Previously, photofabrication has been used principally to make very precise nozzles for ink jet printers. Because of the low aspect ratio and smoothness of the nozzle, the liquid jets have negligible turbulence and monodisperse sprays are easily produced. In Phase I of the contract, we formed photofabricated nozzles with designed perturbations in the nozzle perimeter. Using these designed perturbations, we were able to atomize sheets of fluid and to control the spatial distribution of the resulting spray by varying the acoustic power input.

1.1 Present Spray Technology

The atomization of a jet or sheet of liquid is a process which, in most cases, requires energy to be added to the liquid. The added energy is converted into an increase in surface energy in the liquid as the initial liquid mass is separated into droplets. As the surface area of the liquid increases, the surface energy of the liquid increases. Energy may be supplied for purposes of atomization from either a decrease in kinetic or surface energy of the liquid or from an external source.

1.1.1 Air Blast Atomization

One commonly used process for atomizing a fluid involves impinging a fast moving air stream onto a slower moving fluid, such as a fuel to be burned in a combustor of a turbine engine. With this process, the kinetic energy of the injected air serves to tear the liquid into filaments and then into drops. Thus, a portion of the kinetic energy of the injected air is converted into an increase in surface energy of the atomized fluid.

The instability of the fluid sheet in the air stream is a form of the Kelvin-Helmholtz instability which occurs when layers of fluid are in relative motion [1]. Its use for spray formation has been studied by several researchers [2, 3, 4, 5, 6, 7, 8].

The presently used air injection process, when used to atomize a fuel for burning in a turbine engine, is only effective when the engine is operating, since a source of high-velocity air is needed for atomization. Further, higher engine operating temperatures, which result in greater engine operating efficiency, are difficult to achieve since excess air is added into the engine for purposes of atomization. Additionally, atomization by use of injected air results in an inconsistent distribution of fuel spray in both time and space. As a result, the combustor is required to be longer than otherwise necessary to ensure that all the fuel is burned before the air/fuel mixture exits the combustor. The inconsistent distribution of fuel spray also results in a nonuniform combustion of the air/fuel mixture causing an increase in NOx pollutants being emitted from the engine.

1.1.2 Rayleigh Breakup

A second popular atomization process involves the acoustic excitation of a circular liquid jet at an unstable wavelength. This process, called Rayleigh breakup, is based upon theoretical work by Rayleigh [9], who explained in 1878 that a circular fluid jet is unstable for azimuthally symmetric perturbations whose axial wavelength is longer than the circumference of the jet. The process involves placing small-amplitude velocity perturbations on a circular jet, wherein the perturbations have a wavelength longer than the circumference of the jet. The applied perturbations grow, due to an input of energy from surface tension, and break the jet into a stream of drops at the excitation frequency [10, 11, 12, 13, 14]. Figure 1 is a photograph of an array of six identical jets breaking into a monodisperse spray due to Rayleigh breakup.

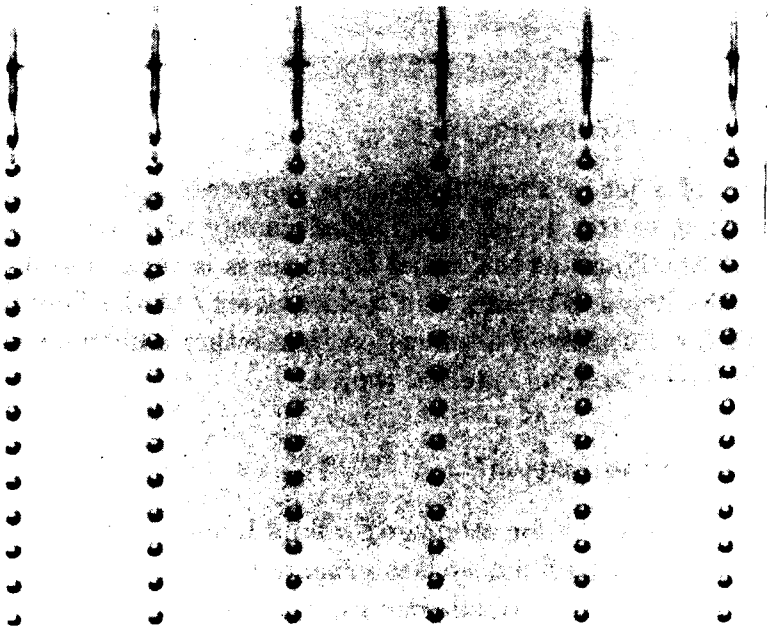

Figure 1. A Jet Array, Driven by Low-Amplitude Velocity Perturbations, Forms a Monodisperse Spray

Rayleigh breakup adds little or no energy to the fluid. Thus, the surface area and surface energy of the fluid are lower after the breakup. Further, the size of the resulting

drops produced by this process have a diameter approximately twice the diameter of the original jet. Thus, if small drops are desired, even smaller nozzles must be used. Small nozzles, however, can be easily obstructed by particles carried by a fluid. Consequently, this process is disadvantageous for use where small droplets are desired. Further, this process will not induce atomization of a sheet of liquid. Due to these limitations, low power acoustic breakup of cylindrical jets has found use mainly for ink jet printing.

1.1.3 Impact Atomization

A third prior atomization process uses the impingement of a liquid jet against a surface or against another liquid jet [15]. This process is used in rocket engines where the fuel and oxidizer streams can be directed at each other to both atomize and mix the two reactants. It is also used in internal combustion engines where the fuel is injected against the hot intake valve. This process is limited in its ability to create a spatially uniform spray and fuel impingement on a hot surface can lead to the buildup of coke deposits.

1.1.4 Needed Improvements in Spray Generators

From this short review of the present spray techniques, we see a need for an apparatus which is capable of adding energy to a liquid stream for purposes of atomization without employing high-velocity air. There is an opportunity to fill this need by employing acoustic energy or kinetic energy for atomizing a round or flat liquid stream into a stream of droplets having a greater surface area and surface energy than that of the initial stream. Additionally, there is need for an atomization apparatus that is not limited to geometries where the fuel jet must impact a flat plate or be directed against another jet.

1.2 Potential Atomization Concepts

1.2.1 Electrodynamic Atomization

John Zeleny [16], Magarvey [17], Huebner [18] and others studied the atomization of fluids by a strong electric field. This process produces small drops that are highly charged. Because of their charge they repel one another and tend to collect on surfaces. That is, clusters of charged drops tend to disperse and move to the boundaries of a volume.

1.2.2 Aerated-Liquid Pressure Atomizers

Lefebvre [19] constructed a novel atomizer that mixes air with the fluid before it is ejected from the orifice. This atomizer has some of the characteristics which are desired in our project. These are the creation of a spray without using a large quantity of air and the creation of small drops from large orifices.

1.2.3 Spatially and Temporally Distributed Excitation

The electrohydrodynamic and magnetohydrodynamic instabilities of liquid jets and liquid sheets were studied because of their similarity to magnetohydrodynamic instabilities in plasma containment devices for thermonuclear power generation.

We used some of these studies to get ideas for driving instabilities on fluid sheets and jets for the purpose of atomization.

Crowley [20] made the $m = 1$ or kink mode of a circular liquid jet unstable by applying a static electric field to the jet. This is the first mode above the naturally unstable varicose mode. Rose and Clark [21] published photographs that show the kink and higher-order magnetohydrodynamic modes on plasma columns. The higher-order modes are star-shaped patterns with the number of points equal to the mode number. These instabilities on cylindrical plasmas are mathematically similar to instabilities on liquid columns and Chandrasekhar [1] places both topics in the same chapter.

The convective nature of the instabilities on cylindrical liquid jets was studied by Melcher and Ketterer [22]. They coupled convecting jets to flexible nonconvecting structures and to other counter-flowing jets. They used the Method of Characteristics and the Method of Bers-Briggs to plot the growth and determine the nature of the coupled instabilities, convective or absolute. Based partly on this work, an educational movie was created for undergraduate students. This movie used cylindrical jets as examples of convective and absolute instabilities [23].

Melcher and Warren [24] controlled a stationary liquid surface, driven unstable by an electric field, by means of an active feedback system. Crowley [25] and Dressler [26] used the convective kink instability of a cylindrical jet or fluid sheet as a model for stabilization studies. Here a fluid jet was controlled by the proper spatial and temporal application of electrodynamic forces.

In these studies of fluid electrohydrodynamic and magnetohydrodynamic instabilities, the idea was to sense the instability, in both space and time. Based on this information, a drive signal was created in both space and time and used to eliminate the instability.

1.2.4 Shock Formation

Another atomization concept that can be used is shock formation. The study of shock formation is most commonly used in gas dynamics and the Method of Characteristics is a mathematical technique frequently employed to model shock formation.

Waves propagating along a cylindrical jet of liquid are mathematically similar to waves propagating in a compressible gas. When a compression wave travels through a gas, the density and pressure increase. On a cylindrical fluid jet, the fluid density is constant and it cannot increase. When a compression wave arrives, the radius of the liquid column and the pressure increase. One can look at a cylindrical liquid column as analogous to a compressible gas, with the pressure-density relationship for the gas replaced by a pressure-radius relationship for the jet.

The amplitude-dependent nature of shock formation is also similar to the high-power acoustic atomization that we have observed in fluid sheets. The low-amplitude compression waves created when people speak, do not steepen into shocks. Large compression

waves, of the type made in shock tubes, do steepen into shocks.

Several previous papers describe applying large perturbations to jets. One of these efforts by Dunne and Cassen [27, 28] succeeded in creating what may be described as a shock on a cylindrical jet and consequently a spray was created. Their drive was not electronic in nature and operated on a single-pulse mode. While their apparatus was not practical for spray generation, they demonstrated the existence of disk formation and breakup on a cylindrical jet.

Crane, Birch and McCormack [29, 30] built a device that almost makes shocks on a liquid jet. Their drive was magnetic and it could produce a periodic drive to the cylindrical jet. It did not have sufficient power to drive a jet of water unstable. They succeeded in driving a paraffin jet, which has a low surface-tension, unstable and drops were ejected radially from the edge of the jet.

Dombrowski [31] succeeded in building a magnetically powered drop generator that drives the varicose modes on a sheet unstable. He used a magnetic transducer to drive a fan nozzle along the axis of the fluid stream.

Dressler [32] mathematically described the atomization of a liquid with shock analysis. This paper shows that the energy of the acoustic drive can atomize a cylindrical jet into drops that are much smaller in diameter than Rayleigh's theory predicts is the smallest drop diameter.

In a similar type of analysis, Sellens [33] and Chin [34] used the concept of entropy to predict the outcome of the atomization process. These last two papers do not consider the energy contribution of an applied periodic drive.

1.3 Development Plan

We combined several of these ideas to develop a drop generator that destabilizes and atomizes liquid jets, shaped as sheets or cylinders, by applying spatially and temporally distributed perturbations. The formation of the atomization is similar to the steepening of pressure pulses in a compressible fluid to form shocks. Perturbations of small amplitude do not steepen to form shocks, but when a disturbance of sufficient amplitude is placed on the liquid, a shock forms and atomization occurs. The atomization is also similar to the atomization produced from impinging jets except here all of the liquid emerges from the same nozzle. Sections of the fluid jet, moving at different relative velocities, collide and the impact atomizes the fluid.

The construction of this commercially useful spray generator requires two developments to be successful. The first is the means to place the temporal perturbations on the fluid jet and the second is the means to place the spatial perturbations on the fluid jet. Both of these perturbations must have sufficient amplitude that the amplitude-dependent instabilities will be created.

Due to temporal and financial constraints, an electrostatic force or aerated liquid will not be used for the drop generator in this project. These methods could be incorporated into the drop generator at a later date.

2 Piezoelectric Driver Design

There are many acoustic drop generator designs published in the literature [35, 12, 13, 36, 37, 38, 39, 40, 41]. Most of these designs are for ink jet printers or other similar devices. That is, they wish to make a monodisperse spray of drops in a single stream. Other designs are for driving an array of jets to produce an array ink jet printer. Since the purpose of these drop generators is to drive the existing Rayleigh instability, the power requirements are small. The acoustic energy is needed only to establish initial conditions for an existing instability. These designs do not supply the power to atomize the liquid.

Magnetic drivers are commonly available and inexpensive. McCormack [29] and Dombrowski [31] used magnetic drivers to drive the nozzles in their experiments. Although their experiments did drive the fluid with enough power to make the amplitude-dependent instabilities visible, the frequency range is too limited and the power requirements are too large for their acoustic drivers to be practical.

We selected piezoelectric elements to provide the motion in our acoustic driver. Piezoelectric drivers have a higher operating frequency than magnetic drivers and thus they provide a more flexible design. The disadvantage of piezoelectric transducers is that the motion of the piezoelectric element is small. To achieve a measurable velocity perturbation in the fluid, the piezoelectric pump must be efficient.

The basic design for a piezoelectric driver is shown in Figure 2. A pair of piezoelectric discs are squeezed against a center electrode by two metal end pieces. This structure is held together by a bolt that passes from one end piece, through the center of the piezoelectric elements and the center electrode, and into a threaded hole in the other end piece.

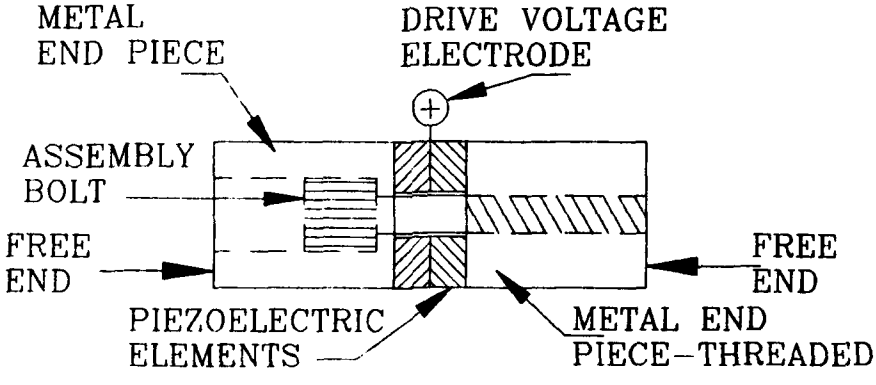

Figure 2. Basic Piezoelectric Driver

The bolt is placed in tension and it supplies the restoring force to return the end pieces to their original position after the structure lengthens due to a voltage signal. The end pieces are electrically connected by the bolt and they are usually held at ground potential. The driving voltage is applied only to the center electrode. By using transducer pairs in

this manner, the high voltage is isolated to the center electrode. Since each end of the transducer is at ground potential, the opportunity for electrical shorts from the unit are reduced.

2.1 Previous Designs

2.1.1 Salt-Shaker Drop Generator

Figures 3 shows how one of the common drop generator designs is made from the basic piezoelectric driver. This design has been described by Rosencwaig [40]and Endo [42] We named this design the Salt-Shaker Drop Generator because of the similarity to the hand-powered device used to eject salt crystals from a nozzle array.

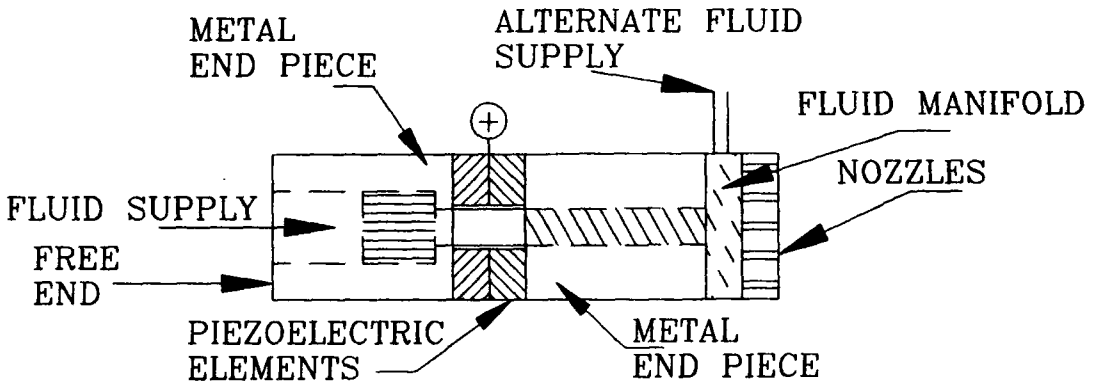

Figure 3. Salt-Shaker Style of Piezoelectric Drop Generator

In the salt-shaker design, the nozzle is rigidly attached to one end of the piezoelectric driver. In this design, the fluid chamber adjacent to the nozzle plate does not change volume when the piezoelectric driver moves. The manifold is accelerated and the sloshing or acceleration of the fluid in the manifold creates pressure fluctuations that drive velocity perturbations on the liquid. It is the inertia of the fluid that leads to the pressure and velocity perturbations.

The acceleration of the nozzle plate is balanced by the acceleration of the free end (other end) of the piezoelectric driver. This salt-shaker should vibrate with the center of mass stationary. The acceleration of the drop producing end is determined by the mass of the entire driver, its geometry, and the its material properties. This design cannot place a static force on material placed in the fluid manifold.

2.1.2 Inertial-Piston Drop Generator

We have named a second common style of piezoelectric drop generator the "Inertial-Piston Drop Generator." A drawing of this style of drop generator is shown in Figure 4.

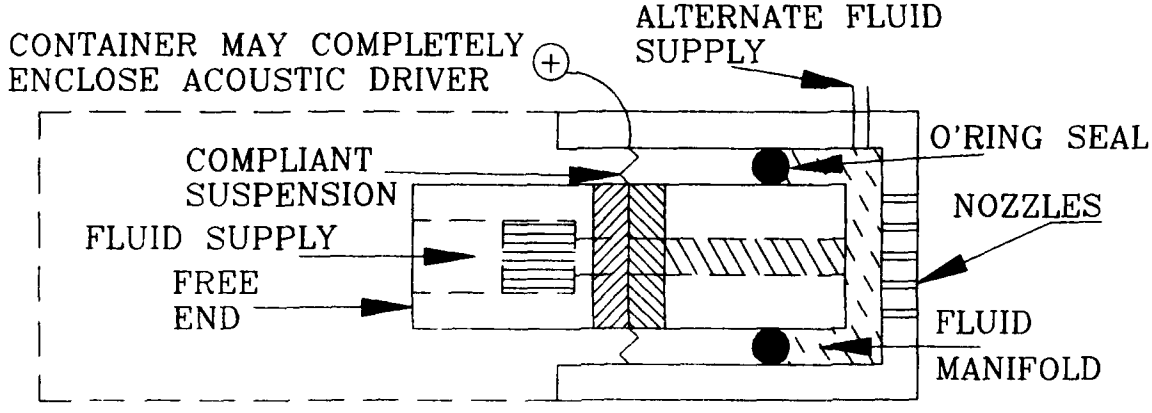

Figure 4. Inertial-Piston Style of Piezoelectric Drop Generator

In the inertial-piston style, the electromechanically-driven piston is mounted through a compliant mount to the nozzle plate. This design differs from the salt-shaker design in that the transducer motion decreases the volume of the fluid manifold adjacent to the nozzle plate. When the piezoelectric material expands, the piston moves as a result of the inertial reaction of the other end of the piezoelectric transducer. The nozzle plate is not attached rigidly to the piston and the manifold volume is decreased due to the relative motion between the piston and nozzle plate.

The mount between the piezoelectric driver and its case or the nozzle plate is compliant. Commercial piezoelectric drivers are suspended inside a case by compliant supports to prevent the case from transmitting high-power acoustic vibrations. In ink jet printers, Cha [38] and Beaudet [39] mounted the piezoelectric drivers in compliant mounts to prevent vibrations in the structure of the printer. In both cases the "give" in the transducer mount limits the compression that can be given to the manifold. The compliant mount also prevents the inertial-piston drop generator from placing a large compression on the manifold when a low frequency or steady voltage is applied to the transducer.

2.2 Phase II Wrap-Around Design

We removed some of the limitations with the older piezoelectric drivers to create a new design that is efficient in creating large velocity perturbations in the fluid. The main limitation of the older designs is that they require inertial forces to generate the motion which leads to an acoustic pressure pulse in the fluid.

The fundamental difference between our new drop-generator design and the older designs is that the new design does not require inertial forces, although it often makes use of them. The new device has no compliant mounts or "give" to it. The new device has no free end which will eventually move to relieve any pressure. It can statically squeeze the fluid chamber and make huge pressure increases while the others cannot.

If a solid material was placed into the manifold of the other drop generator designs and a dc voltage applied to the piezoelectric driver (or magnetostrictive driver), there would be a compression at the instant the voltage was applied. In the Cha [38] and Beaudet [39] designs, after the initial transient pulse, the mounts for the acoustic driver would flex, reducing the compression force to a low value. In the salt-shaker designs, the compressive force would quickly decay to zero.

If a solid was placed into the fluid manifold of this wrap-around drop generator (the solid would exactly fill the volume that existed when the voltage on the piezoelectric elements was zero) and a dc voltage applied to the piezoelectric unit, a steady compression would be applied to the solid. The compression would last as long as the voltage remained on the electrodes. The compressive force could also be large.

The basic design of the Phase II piezoelectric driver is shown in Figure 5. The piezoelectric driver is a long structure with a cap at one end and a piston at the other. The nozzle plate is attached rigidly to the cap end of the piezoelectric driver by a hollow tube and the piston is located adjacent to the nozzle plate. This configuration squeezes the layer of fluid located between the piston and nozzle plate. The acceleration of the fluid to the periphery of the fluid manifold creates a pressure increase in the manifold center. The increased manifold pressure creates a velocity increase in the fluid ejected from the nozzle.

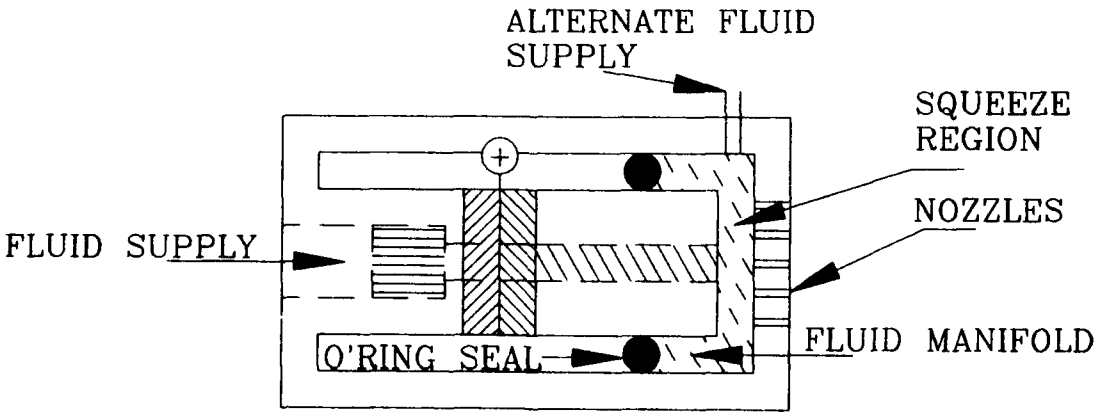

Figure 5. Wrap-Around Style of Piezoelectric Drop Generator

There is no free end on the Phase II piezoelectric driver. One end of the driver is the piston and the other end has been wrapped over the outside of the piezoelectric driver

and fastened directly to the nozzle plate.

Our design can be compared to a C clamp. The nozzle plate is the clamping surface fixed at one end of the C. The fluid piston is the clamping surface located at the end of the screw. In a normal C clamp, the two surfaces are forced together when the screw is tightened. In the drop generator, the two clamping surfaces are forced together when the piezoelectric transducer increases in length due to an applied voltage.

The final design also has a thin gap around the circumference of the driving piston. This thin gap helps to get sufficient pumping action during operation.

A photograph of a disassembled drop generator is shown in Figure 6.

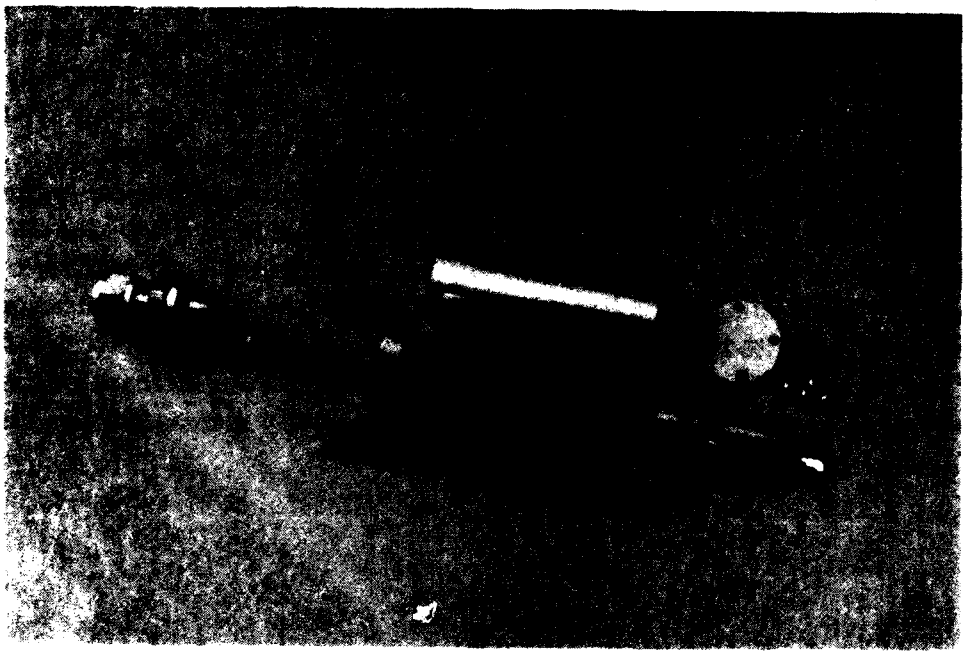

Figure 6. Photograph of 1 Inch Diameter Piezoelectric Drop Generator

3 Nozzle Plate Design

3.1 Present Bimetal Nozzle Construction Method

The current bimetal nozzle plate manufacturing technology is described by Gamblin [43] and by Wallace [44]. Wallace describes the standard bimetal process for making nozzle plates and his intended use was the Liquid Drop Radiator(LDR) Project. Gamblin describes a variation that uses corrosion resistant materials to make nozzles for spraying textile dyes. This process is a slight modification for making evaporation or exposure masks [45, 46]. The fabrication technique is often called "electroforming," after the formation of the nickel nozzle by electroplating over a mandrel, or "photofabrication," after the use of photoresist to define the nozzles. The process was probably first used for ink-jet-printer nozzle plates in 1970 by the Buckbee-Mears Company of St. Paul, Minnesota. Figure 7 illustrates the steps in the bimetal process.

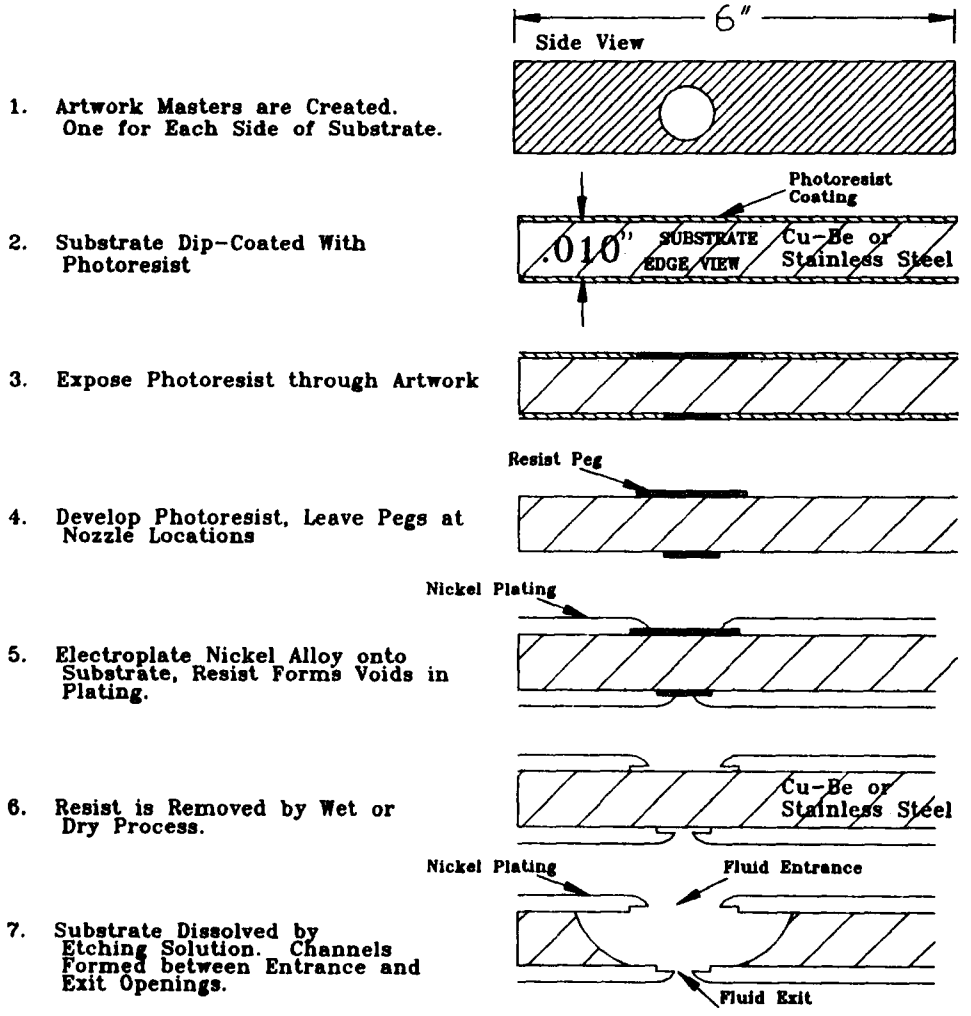

Figure 7. Standard Process for Manufacturing Bimetal Nozzles

The first step in bimetal nozzle plate production is the creation of a photographic plate that defines the desired hole shape and placement as well as the nozzle plate boundary. These photographic plates are generated by computer controlled plotters.

The second step is to coat both sides of the substrate with photoresist by means of a dip coater.

Third, the photoresist is exposed to ultraviolet light through the photographic plates. This polymerizes the resist in those locations where a nozzle will be located in the finished nozzle plate .

Fourth, the resist is developed by spraying the plate with a solvent that washes away the unpolymerized photoresist, leaving spots of developed resist, called "pegs," on both sides of the substrate. The pegs are formed in registered pairs; each peg has a corresponding peg on the opposite side of the substrate.

Fifth, nickel is electroplated onto the substrate. The resist pegs are insulating and therefore the electroplating does not occur at their locations. The nickel plating is made thick enough to totally enclose the sides and partially cover the tops of the resist pegs. The resist peg has an extremely smooth top surface and it makes the nickel surface around the nozzle very smooth. This smooth nickel surface surrounding the nozzle hole is the reason the bimetal nozzle plates produce turbulence free jets.

In the sixth step, the resist pegs are removed by a solvent, leaving the substrate with a cladding of nickel. The nickel cladding has holes exposing the substrate at the former locations of the resist pegs.

For the seventh step, the bimetal plate is then immersed in an etchant which dissolves the substrate and does not dissolve the nickel. The etchant opens the nozzles by cutting through the substrate at the locations of the hole-pairs in the nickel. The nickel is considered to be a protective mask or resist for the etchant; only the substrate exposed by the holes in the nickel is etched.

This bimetal process will work with many materials and etchants. The key to the process is the selection of a plating bath, substrate, and etchant whereby the etchant will dissolve the substrate and not react with the plated metal.

Figures 8 and 9 show photographs of a typical round nozzle as seen from a microscope. In the left image, the microscope is focused on the outside surface of the fluid entrance hole. In the right image, the microscope has been focused on the inside surface of the exit hole. The ring surrounding the exit hole is the smooth imprint of the photoresist peg in the nickel plating. Outside the smooth peg mark, there are scratches in the nickel plate. These scratches were initially in the substrate surface and they have been transferred to the nickel plating.

Figure 9 also shows that the entrance hole to a bimetal nozzle is usually made much larger than the exit hole of the nozzle. This is done to minimize the influence of the entrance holes on the resulting flow from the nozzles. When fluid is pumped through the nozzles in the bimetal plate, the liquid flow is principally determined by the higher resistance of the exit hole due to its smaller diameter.

Ink jet printing requires quiet jets, that is, jets with no turbulence. This application requires jets that are steady, break into drops at the driving frequency, and do not produce satellites. For textile printing, the minimization of turbulence in the liquid jet

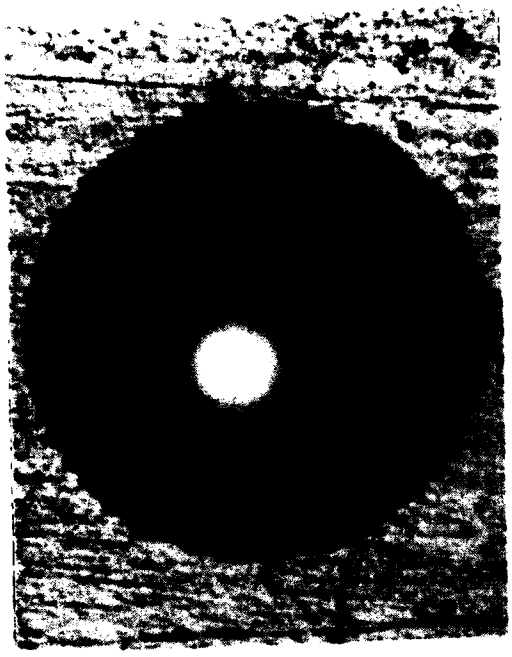

Figure 8. Round Fluid Entrance Hole, View Focused on Entrance Surface

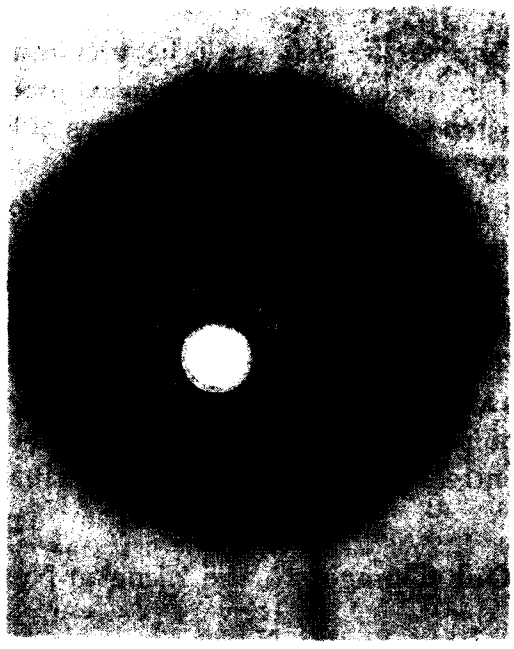

Figure 9. Round Fluid Exit Nozzle, Viewed through Fluid Entrance Hole

is extremely important since the droplet streams must travel long distances. If there is turbulence in the liquid flowing from the nozzle, then the drops formed from the stream will not have identical velocities. Some will collide and coalesce if they travel for long distances, due to the fast drops overtaking the slow drops.

Ink jet printing also requires jets that are extremely parallel. If the jets are not parallel, there will be errors in the aiming of the jets and the printing will be distorted. To achieve the required accuracy, great care is taken to register the resist peg pairs on opposite sides of the substrate. Even when the entrance hole is much larger than the exit hole, misregistration of the holes can cause a small deviation in the trajectory of the jet. Figure 9 shows why the bimetal nozzles are the preferred method for parallel and nonturbulent jets. The nozzle exit hole has a mirror finish surrounding it. Each nozzle has an entrance cavity which serves to channel the fluid to the exit nozzle and block the influence of adjacent nozzles. Although the pictured nozzle does not have perfect alignment, the entrance hole can be registered precisely with the exit hole so that the entrance holes do not cause misalignment in the fluid streams.

3.2 Requirements for Nozzles for the Acoustic Drop Generator

In contrast to the bimetal nozzles, commercial fuel spray nozzles for oil burners or turbine engines usually produce large amounts of turbulence in the fluid stream to help initiate the atomization process. These commercial nozzles are made from tubes or slots with large length-to-diameter ratios. The induced velocity profile creates turbulence which helps to tear the fluid stream into small drops [47, 48].

For our method of producing drops of liquid by means of a large velocity perturbation,

we require nozzles that are in between commercial spray nozzles and precision bimetal nozzles in the quantity of turbulence produced. The desired nozzles for the acoustic drop generator should produce streams of liquid that have a small amount of controlled vorticity.

We additionally need nozzles which form sheets that maintain their shape while travelling away from the nozzle. When a liquid sheet is formed at a simple slot, the sheet tends to collapse to a round stream due to the surface tension. This collapse to a cylinder places the fluid into a lower surface area configuration and is undesirable for atomization [3, 49].

We also need nozzle plates that form diverging jets. The jet arrays for ink jet printers must be parallel for printing accuracy. The jets from our drop generator should diverge in a controlled manner to spatially distribute the spray.

3.3 Our Changes to the Bimetal Nozzle Manufacturing Process

3.3.1 Rectangular Nozzles

Figure 10 shows a photograph of a simple nozzle designed for this contract. This nozzle is seen looking through the bimetal plate from the fluid entrance hole. The rectangular resist peg mark surrounds the nozzle. The entrance hole is large and out of focus in this view. This nozzle was manufactured to form a rectangular fluid jet or sheet.

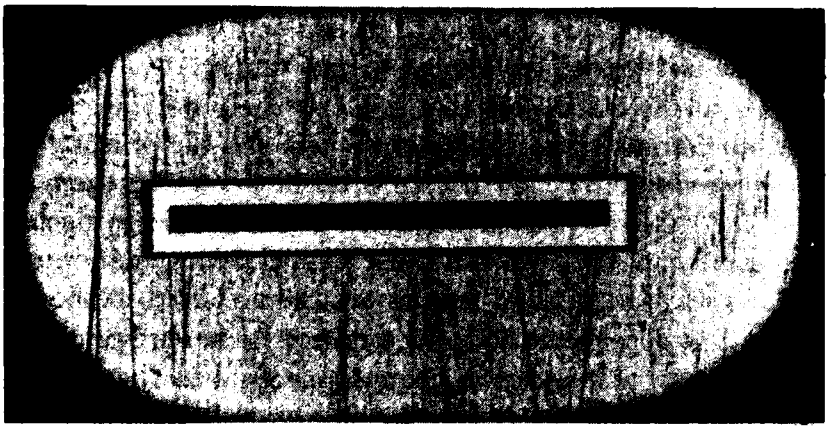

Figure 10. Rectangular Slot. 500 x 50 Microns

3.3.2 Perturbations in Nozzle Perimeter

Figure 11 shows a more complicated nozzle. Here a slot has been modified by placing notches in its sides. These notches produce thickness variations in the fluid sheet and we refer to these thickness variations as spatial perturbations. The amplitude of these spatial perturbations is independent of time and the perturbations have a wavelength that is fixed by the spacing of the notches.

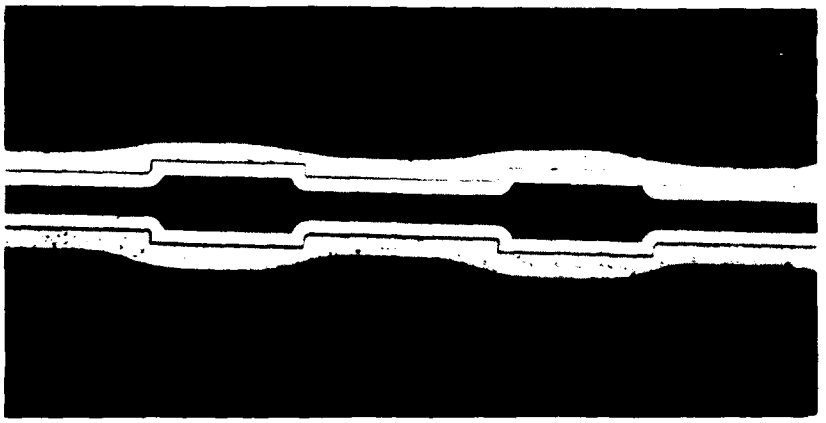

Figure 11. Rectangular Slot with Width Perturbations. These notches create spatial perturbations in the fluid sheet.

3.3.3 Offset Entrance and Exit Holes.

The typical uses for bimetal nozzles require parallel fluid streams and the entrance and exit holes are precisely registered to obtain this parallelism.

For fuel sprays, it is desirable to have the streams of liquid diverge so that the spray will uniformly fill the volume of the combustor. Based on this requirement for non-parallel streams, nozzle plates have been constructed with the entrance and exit nozzles offset or "misregistered" in a controlled manner. Figure 12 is an example of a round nozzle with extreme misregistration of the entrance and exit holes. This process of

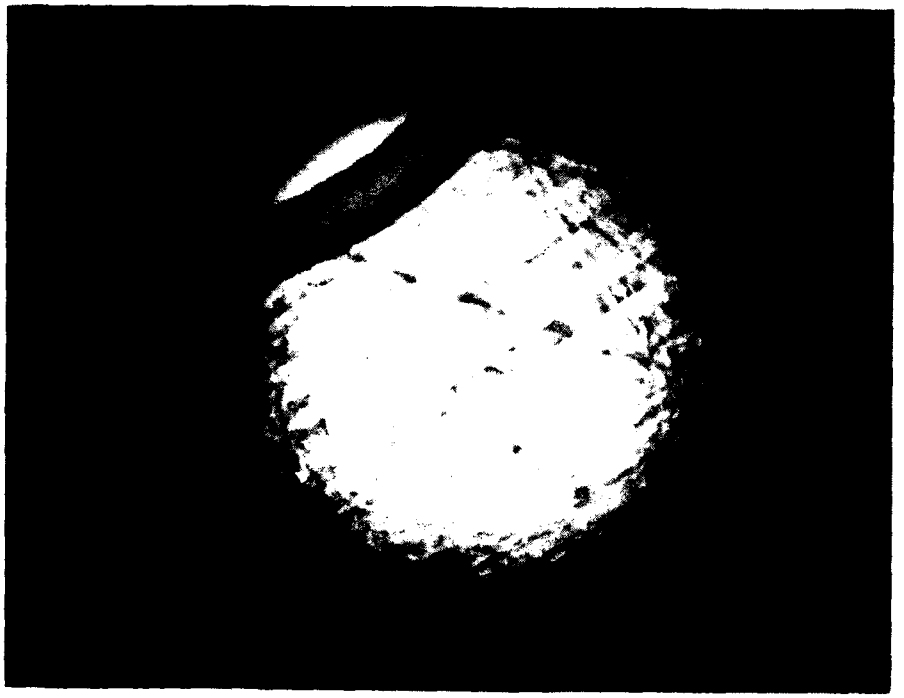

Figure 12. Round Nozzle with Entrance and Exit Holes Misregistered. The edge of the exit nozzle is visible through the top of the entrance hole.

This process of deliberate misalignment can be used on nozzles of any shape. Figures 13 and 14 show a rectangular nozzle which has the entrance and exit openings of approximately equal size. The slots are offset so only the notched edge of the exit slot is visible through the entrance slot.

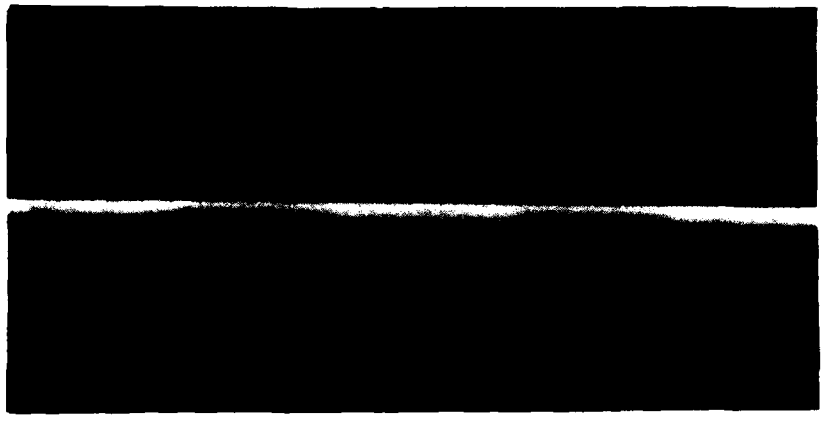

Figure 13. Top-Focus View of Notched Slot Nozzle with Entrance and Exit Holes Misregistered

Figure 14. Exit-Focus View of Notched Slot Nozzle with Entrance and Exit Holes Misregistered

3.3.4 Size Adjustment of Entrance Hole

The dimensions of the fluid entrance hole can be made similar to or smaller than the dimensions of the exit hole. This will allow the entrance hole to have a noticeable effect on the flow from the exit hole.

This idea is particularly useful for rectangular nozzles. When fluid sheets are formed by rectangular nozzles made by the typical bimetal process, the sheet tends to collapse into a round jet. This is shown in Figure 28, which appears in Section 5.3.1.

This sheet contraction can be prevented if the entrance nozzle is made shorter than the exit nozzle. The exit sheet will then have velocity components which spread the sheet as it travels from the nozzle plate.

The drawing in Figure 15 shows a nozzle design that will produce a sheet which expands after leaving the nozzle. The entrance slot is shorter than the exit slot and this geometry gives the fluid at the sheet edge an outward component.

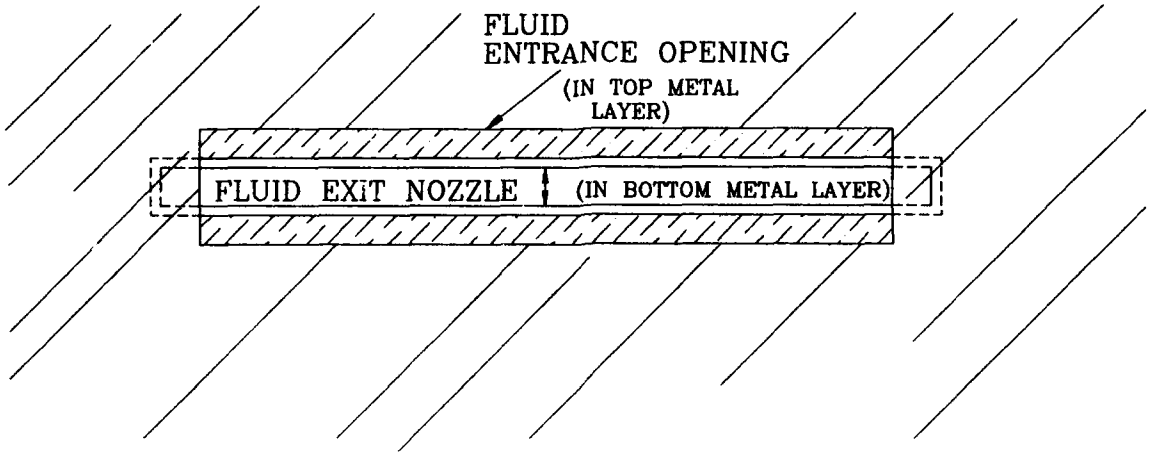

Figure 15. Drawing of Rectangular Nozzle with Short Entrance Hole.

3.3.5 Rotation of Entrance and Exit Holes

Another idea, similar to offsetting the entrance and exit holes, is to rotate the entrance and exit holes with respect to one another. This idea is used principally on rectangularly shaped nozzles and it compliments the idea presented in Section 3.3.4. This nozzle rotation puts a twist into fluid sheets and serves to prevent the sheet from collapsing into a round stream.

Figures 16 and 17 show two examples of rectangular nozzles with rotated entrance and exit holes.

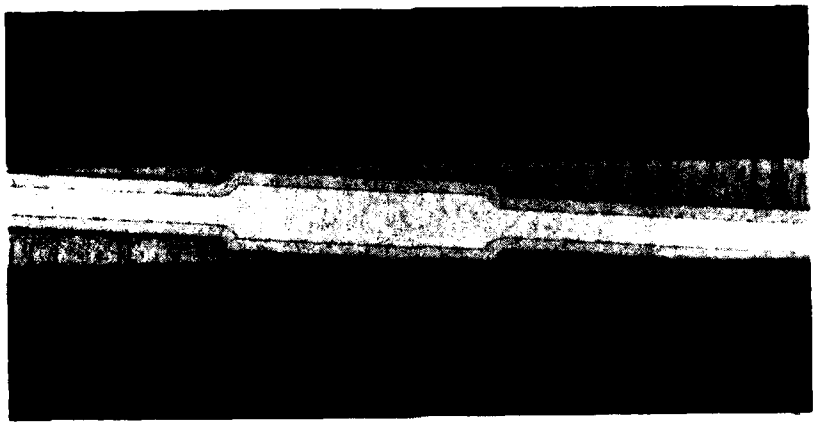

Figure 16. Rotated Rectangular Entrance and Rectangular Exit Slot with Width Perturbations. This rotation creates a twisting sheet.

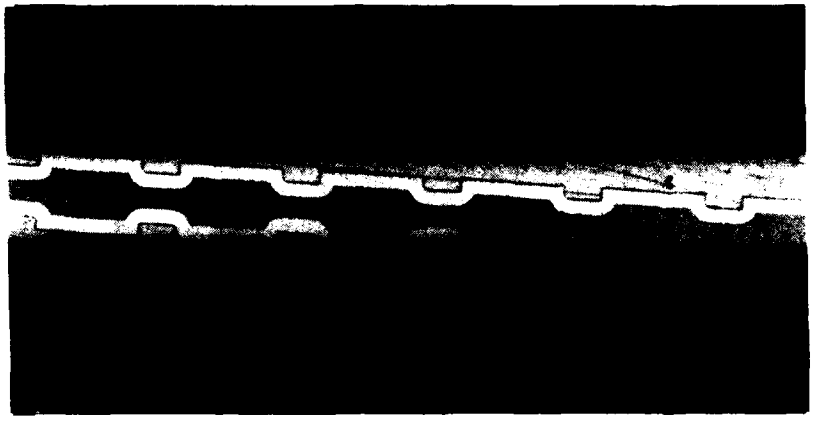

Figure 17. Rotated Rectangular Entrance and Exit Slot with High-Frequency Width Perturbations

3.4 Etched Nozzles from Single Layer Stainless Steel

3.4.1 Cross-Shaped Nozzle

Photofabrication techniques can also produce nozzle plates that are not as precise and smooth as the bimetal plates but which are still suitable for some applications.

The simplest process requires only a few steps. An artwork is made for the nozzle plate borders and nozzle holes. A sheet of stainless steel is coated with photoresist and the resist is exposed through the artwork and developed. After development, the stainless steel is covered by resist except where nozzles and the part edges are to be located.

The part is then placed in an etchant which dissolves the exposed metal and makes holes at the desired nozzle locations.

A plate made by simply etching a sheet of stainless steel is shown in Figure 18. This hole, etched through the stainless steel sheet, is not as precise as the bimetal photofabricated holes. The surface adjacent to the hole is rough, the sides of the hole are not parallel, and the hole is not as symmetrical as a bimetal hole.

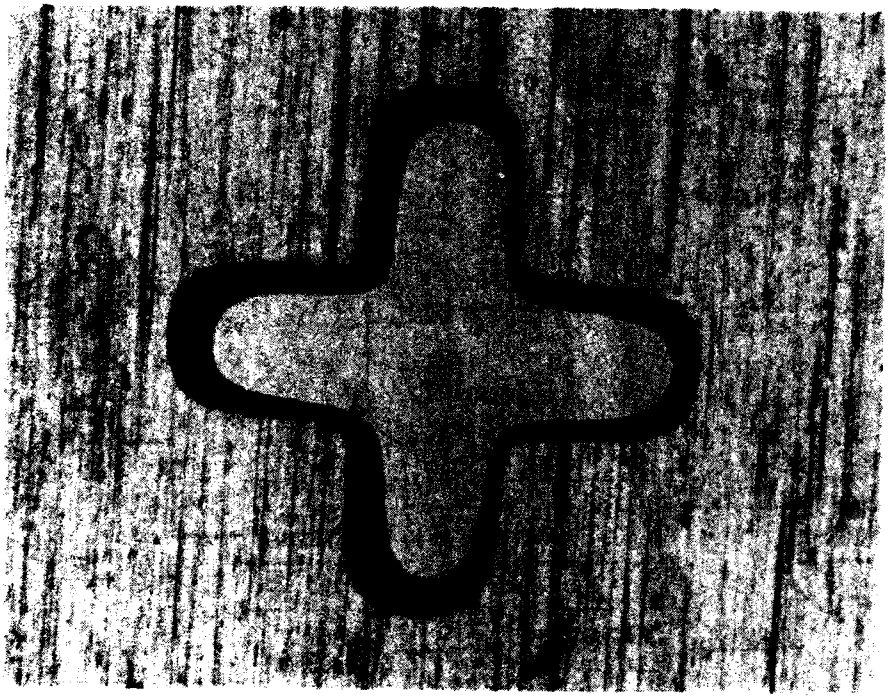

Figure 18. Cross-shaped Nozzle in Single-Layer Stainless Steel. These notches create spatial perturbations on a cylindrical fluid jet.

4 Description of Apparatus

Figure 19 is a block diagram of the total droplet generator. Compressed air forces liquid from the supply tank to the fluid manifold located in the drop generator head. The manifold is closed on one side by the orifice plate. A pressure gauge, located in the manifold, monitors the static pressure of the fluid adjacent to the orifice plate. Controlling the manifold pressure adjusts the flow of liquid through the orifices.

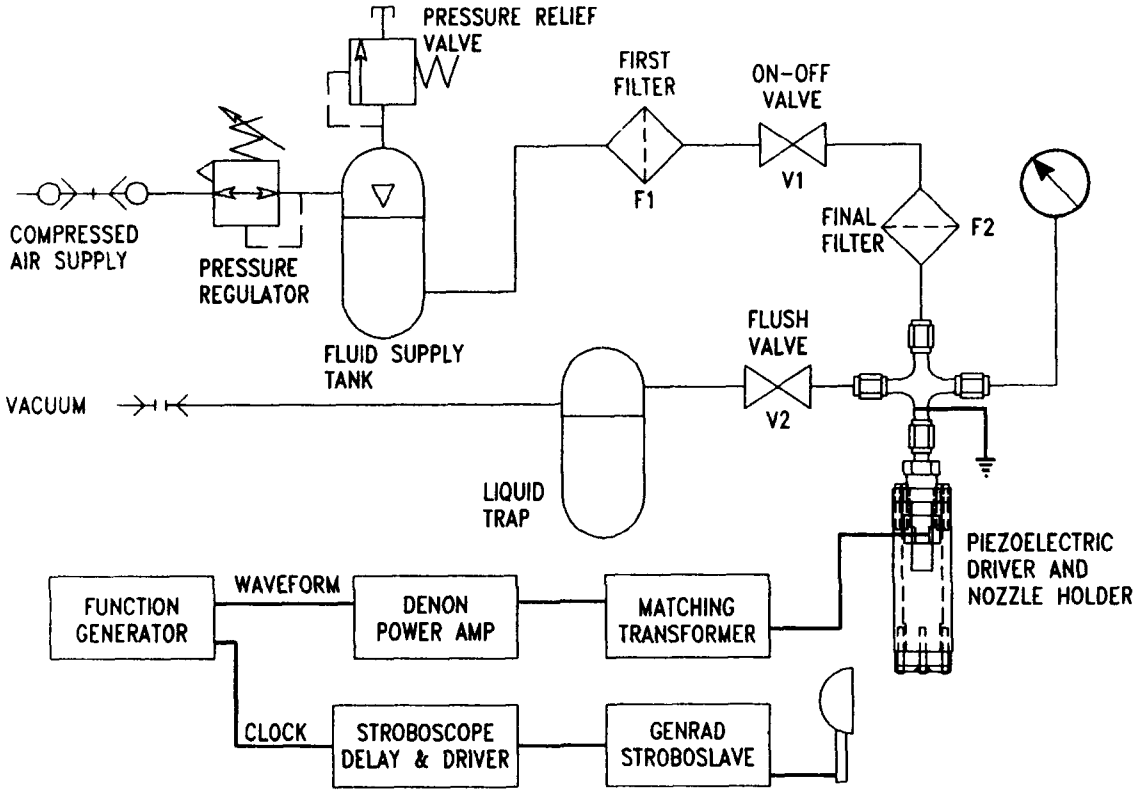

Figure 19. Schematic of Experimental Apparatus

There are two filters in the fluid line between the fluid supply tank and the fluid manifold. The first filter, F1, is a high-dirt-capacity depth filter with a nominal rating of 0.8 micron. It traps most of the particles that are larger than 0.8 micron and it collects some percentage of smaller particles. This filter is a depth filter, that is, it traps particles throughout the volume of the filter material. Because the filter has a large volume for particle retention, it can clean a large volume of fluid before it becomes plugged and must be replaced.

The second filter, F2, has an absolute rating of 3 microns and it is a membrane filter. It traps particles only on its surface. This filter material can trap only a small amount of particles before it becomes plugged and must be replaced.

The second filter, F2, is required to catch fibers of filter material that are shed from the first filter, F1. The polypropylene filter cartridges that are used for F1 are considered

to be nonshedding by their manufacturers. However, our application is more demanding than the normal application for these filters and these "nonshedding" filters do shed some material that will plug the nozzle of the drop generator.

The second filter is also required to remove particles that are generated when Valve V1 is operated. The fittings on the fluid supply line after F1 can also shed a few particles that F2 catches.

A membrane filter can be used alone and it will provide satisfactory filtering for the drop generator. The disadvantage of operating with only a membrane filter is that it becomes plugged frequently.

An exhaust valve located on the drop generator head allows filtered fluid to be flushed through the manifold. Flushing the manifold before starting the drop generator helps remove dirt that can block the orifices. The exhaust valve is closed during normal operation.

The stimulation system which includes the function generator, a Denon power amplifier with a matching transformer, and the piezoelectric transducer, drives axial velocity perturbations on the jet. The function generator also provides a variable clock signal for the stroboscope synchronizer. The driving signal is then amplified by the Denon power amplifier and sent through a matching transformer to the piezoelectric transducers. The piezoelectric transducers generate pressure variations in the fluid manifold which make velocity perturbations on the liquid jets. If the jet is unstable at the wavelength and amplitude of the velocity perturbations, then it breaks into drops at the frequency of the stimulation signal.

A stroboscope and synchronizing circuit are normally used with the drop generator. The high-speed light flashes in synchronism with the acoustic jet stimulation signal and creates a stationary image of the drop formation process.

5 Test Results

The drop generator was operated with a variety of nozzle plate configurations and over a broad range of acoustic power levels. It was operated at low power levels for Rayleigh breakup and at power levels that demonstrated the existence of amplitude-dependent instabilities.

5.1 Experiments on Circular Jets: Rayleigh Breakup

In Phase I of this contract, we demonstrated the flexibility of the bimetal photofabrication process by making a wide range of bimetal nozzle configurations. The Phase I report documents the many different nozzle arrays that were constructed and how these plates operated in the Rayleigh breakup regime.

During Phase II, we built only those configurations which demonstrate some unique qualities of the drop generator when operated in the Rayleigh regime.

5.1.1 Smallest Nozzle and Highest Frequency

This experiment was conducted to establish how small we could make nozzles and still be able to operate them. The experiment was also conducted to operate the drop generator at the highest available frequency. The drop generator used a nozzle array of six nozzles, located in a line. The spacing between nozzles was 1000 microns and the nozzle diameters alternated between 8 microns and 18 microns. Figure 20 is a photograph of this test. The

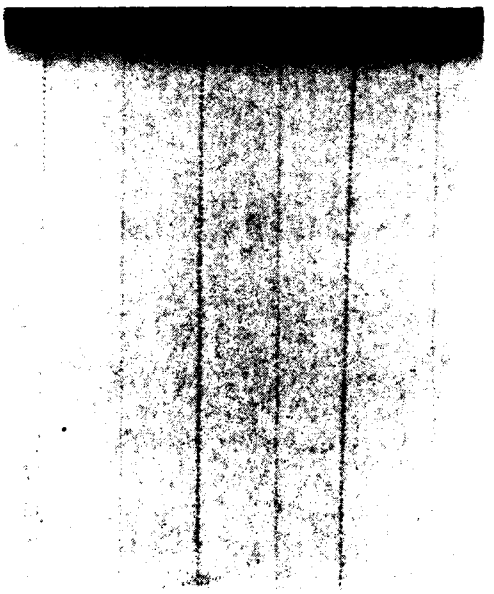

Figure 20. A Jet Array of Alternating 8 and 18 Micron Diameter Jets, is Acoustically Driven at 220 kHz

nozzles were well formed and there was no significant plugging problem from particles in the fluid. From this test, it can be concluded that nozzles with diameters smaller that eight microns could be operated.

This test established 220 kHz as the highest frequency at which the drop generator can operate due to the bandwidth of the acoustic amplifier and coupling transformer. At frequencies above 220 kHz, almost no power is available from the amplifier.

5.1.2 Nine Jet Parallel Array for Evaporation Studies

A nozzle plate was prepared with a nine-hole array, arranged as a 3x3 square pattern. The hole diameter was 40 microns and the hole-to-hole spacing in a row or column was 500 microns. This plate was prepared for evaporation studies. The evaporation of a drop on the exterior of the array could be compared to the evaporation of a drop from the center jet. This data would show the influence of the surrounding jets on the evaporation of the center jet.

For this test, the jets must be parallel so the drop array stays together as the drops travel from the nozzle plate. A photograph of the jet array is shown in Figure 21 and no noticeable divergence of the streams is visible.

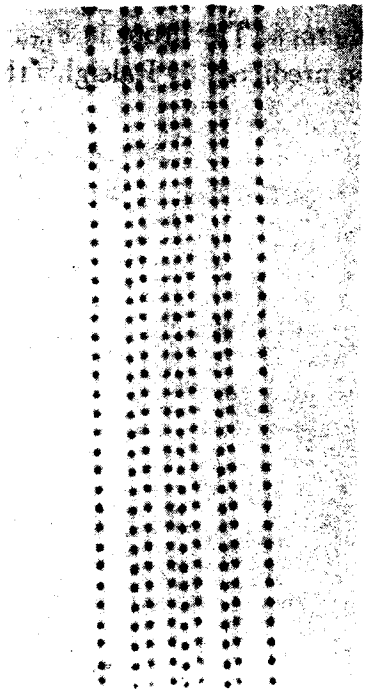

Figure 21. A 3x3 Square Array of 40 Micron Diameter Jets is Broken into Drops at 99.3 kHz

5.2 Experiments On Circular Jets: Amplitude-Dependent Instabilities

5.2.1 Zero Order Azimuthally Symmetrical Mode (Sausage or Varicose)

According to Rayleigh's theory, wavelengths shorter than the circumference of a jet are stable. This theory was derived using the assumption that the initial perturbation was infinitesimal and provided no energy for the jet breakup. The shock theory we have

derived for large perturbations says that the jet can be unstable if the acoustic drive provides the energy required to create the small drops.

A demonstration was conducted to illustrate Rayleigh's theory and also to demonstrate that the jet can be atomized when acoustic energy is added as our theory predicts. A nozzle plate producing a linear array of eight jets was used.

This test also demonstrates some of the capability of our piezoelectric driver design to produce large amplitude velocity perturbations on the jet.

Figure 1 shows a jet array that is unstable for the applied perturbation. The varicose disturbances grow in amplitude as the jets move from the top to bottom of the photograph. This process for jet disintegration is commonly called Rayleigh breakup.

Figure 22 shows a jet that is stable for the applied perturbation. The wavelength of the perturbation is smaller than the jet circumference and the perturbation decays as the jet moves from top to bottom of the photograph.

Figure 23 shows the jet of Figure 22 driven with a larger amplitude signal. With the higher acoustic signal, the jet is unstable and breaks into a stream of drops at the driving frequency. For this jet, the Rayleigh wavelength is 314 microns. The wavelength of this disturbance is about 280 microns. The drops in Figure 23 have a volume that is 10 percent less than the smallest drop predicted by Raleigh's theory for small perturbations.

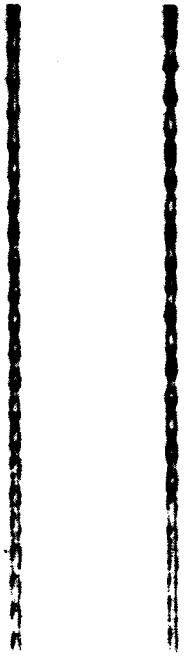

Figure 22. Circular Jet Exhibiting Decaying Perturbations

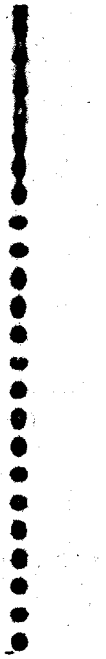

Figure 23. Circular Jet Exhibiting Amplitude-Dependent Instability

5.2.2 Higher Order Azimuthal Modes

Rayleigh's theory predicts that the higher order modes of a liquid cylinder are stable for small perturbations. We have succeeded in driving a jet of liquid unstable in the higher

modes by the application of a high-amplitude acoustic drive. Again, this instability is dependent on the amplitude of the excitation. Figure 24 shows a liquid jet from a nozzle of 750 microns diameter with radial perturbations that are created by our acoustic excitation. These perturbations do not exceed the stability threshold and they decay as the jet moves. Figure 25 shows the same jet with a larger initial perturbation. These perturbations exceed the stability threshold and the jet is unstable, ejecting drops in the radial direction. There are 14 to 16 drops ejected from each perturbation on the jet and therefore we must be driving the $m = 14$ or $m = 16$ azimuthal mode.

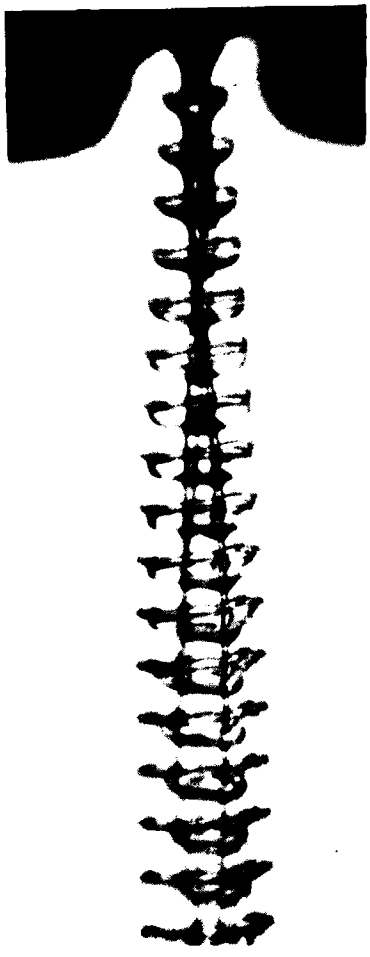

Figure 24. Stable Perturbations on a 750 Micron Circular Jet

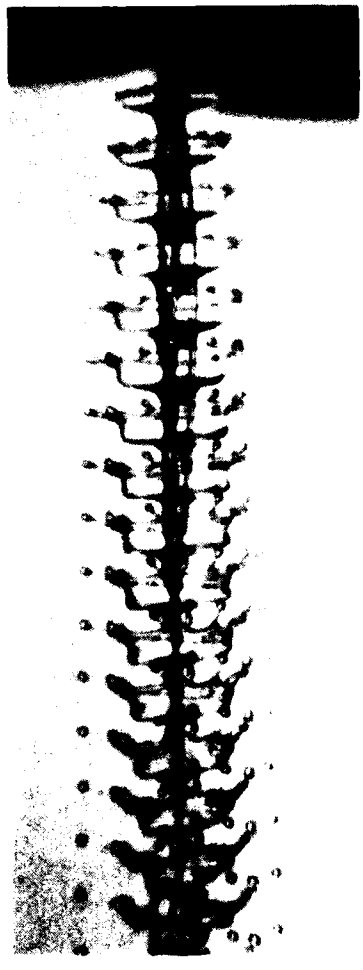

Figure 25. Unstable High-Order Perturbations on a 750 Micron Circular Jet

The same experiment was conducted with a nozzle of 200 microns diameter and the resulting spray formation is shown in Figure 26. The smaller jet diameter created a spray that appeared slightly different than the jet in Figure 25.

A drilled ruby nozzle of 50 microns in diameter was fixed to the piezoelectric driver and it also operated at the high-order breakup mode. The high-amplitude acoustic atomization of the 50 micron jet is shown in Figure 27.

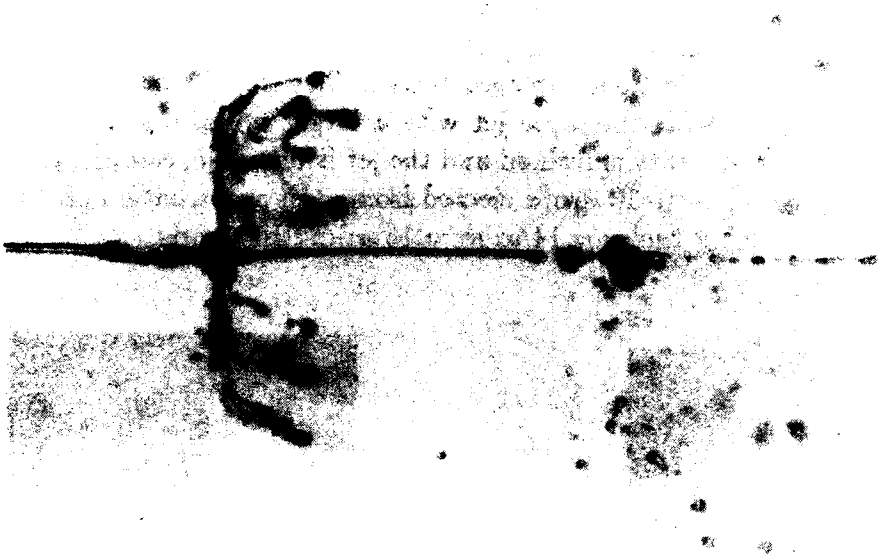

Figure 26. A Jet from a Nozzle of 200 Microns Diameter is Broken into a Spray at 5.2 kHz

Figure 27. A 50 Micron Jet from a Drilled Ruby Nozzle is Broken into a Spray at 24 kHz

5.3 Sheet Instability From A Single Layer Rectangular Nozzle

5.3.1 Stable Spatial and Temporal Perturbations on a Sheet

Figure 28 is a photograph of a liquid sheet originating from a slot nozzle. Small temporal perturbations are applied to the nozzle by acoustically perturbing the fluid velocity. Spatial perturbations are applied to the sheet thickness by putting perturbations in the nozzle width as shown in Figure 11. Figure 28 shows the sheet is stable for these specific perturbations. The sheet was also stable for all other small perturbations.

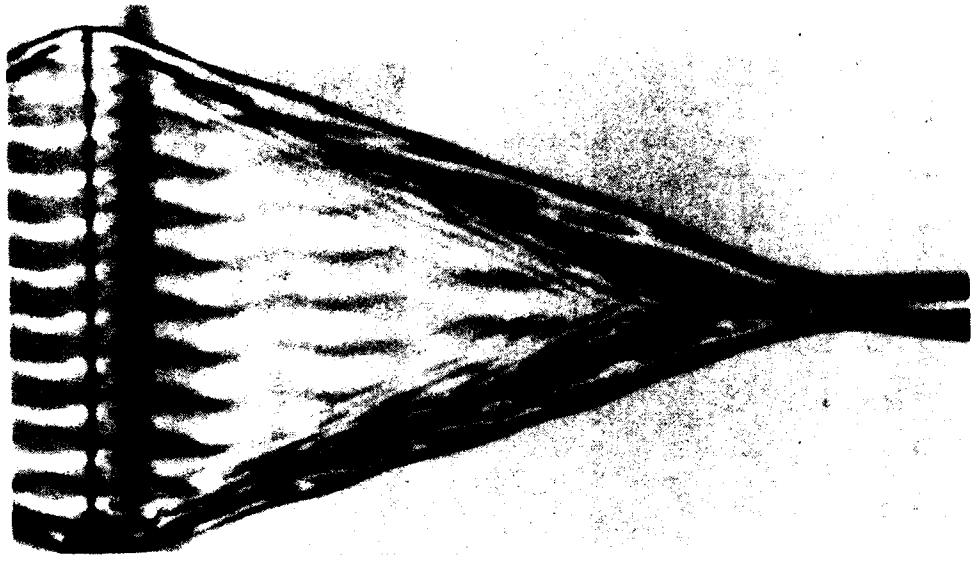

Figure 28. Sheet of Fluid Exhibiting Stable Perturbations

5.3.2 Varicose Instabilities on a Fluid Sheet

Figure 29 shows the sheet after it was made unstable in the thickness mode. A large acoustic signal is applied to the sheet and it breaks into tubes as a result of this large signal. Since a large excitation is required to produce this sheet-breakup mechanism, this instability is called amplitude dependent. The nozzle used for Figure 29 is similar to the nozzle shown in Figure 11. This nozzle contains thickness perturbations which produce perturbations in the tube diameter and induce the tube to break into drops by the familiar Rayleigh breakup.

5.3.3 Kink Instabilities on a Fluid Sheet

The higher-order azimuthal modes on the circular jet were shown to have an amplitude-dependent instability. For this instability, drops were ejected radially from the jet. Similarly, the second order or kink modes of the sheet can be forced to become unstable if

driven with a large enough amplitude. Figure 30 shows ligaments of liquid extending from one side of a sheet due to the application of an acoustic driving force. If these perturbations are not large enough to be unstable, they can collapse back into the sheet. When a sufficiently large perturbation is applied to the sheet, the perturbations become unstable and drops are ejected from the ends of the fluid ligaments as shown in Figure 30.

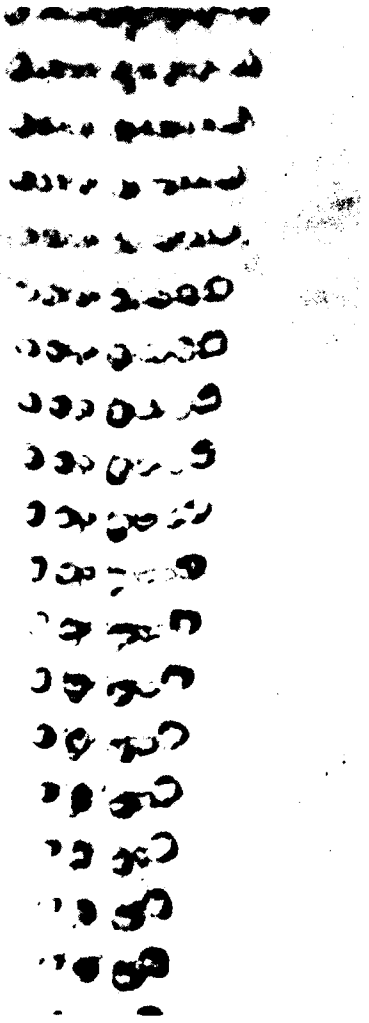

Figure 29. Sheet of Fluid Unstable in the Thickness Mode at 14.6 kHz, Tubes Then Break into Drops

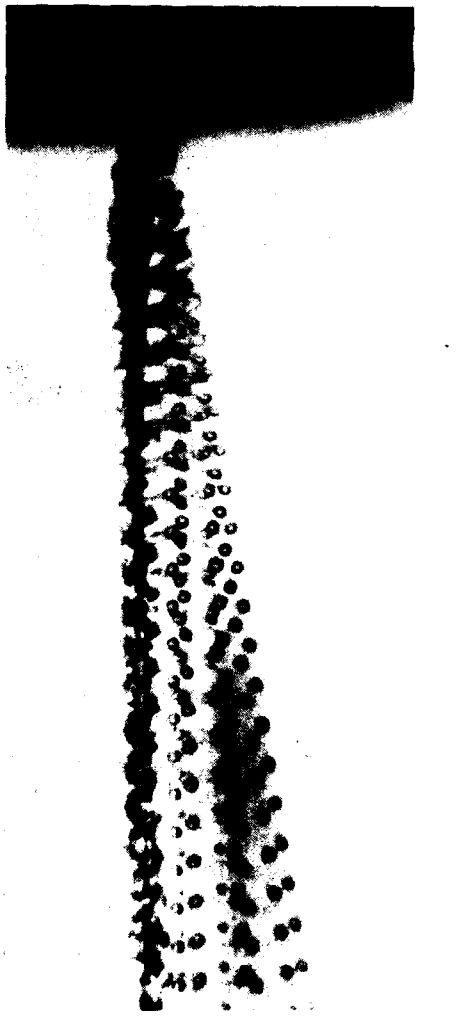

Figure 30. Amplitude-Dependent Instability, High-Order Kink Modes on a Fluid Sheet, Side View

5.4 Sheet Instabilities From A Complex Nozzle

5.4.1 Sheet Deflection from Offset Entrance and Exit Holes

In Section 3.3.3, nozzle plates were described that had both nickel layers configured to influence the fluid jet. Experiments were made using the nozzles of Section 3.3.3 and the results are shown here. Figure 31 shows an edge view of the sheet after it emerges from the nozzle. The photograph shows that the fluid stream has been deflected from perpendicular by about 15 degrees. Figure 32 shows the same stream atomized with an acoustic drive.

Figure 31. Sheet of Fluid Emerging from a Slot with an Offset Entrance Hole

Figure 32. Driven Sheet of Fluid from Slot with Offset Entrance, 10.2 kHz

The experiment was tried again with a fluid whose viscosity was 10 cps. Here the behavior of the fluid is noticeably different. When the low viscosity fluid was used, the complex nozzle structure apparently created turbulence in the fluid and this turbulence affected the sheet atomization. In Figure 33 the increased viscosity damps the turbulence and the behavior of the stream is significantly less turbulent when there is no acoustic drive applied.

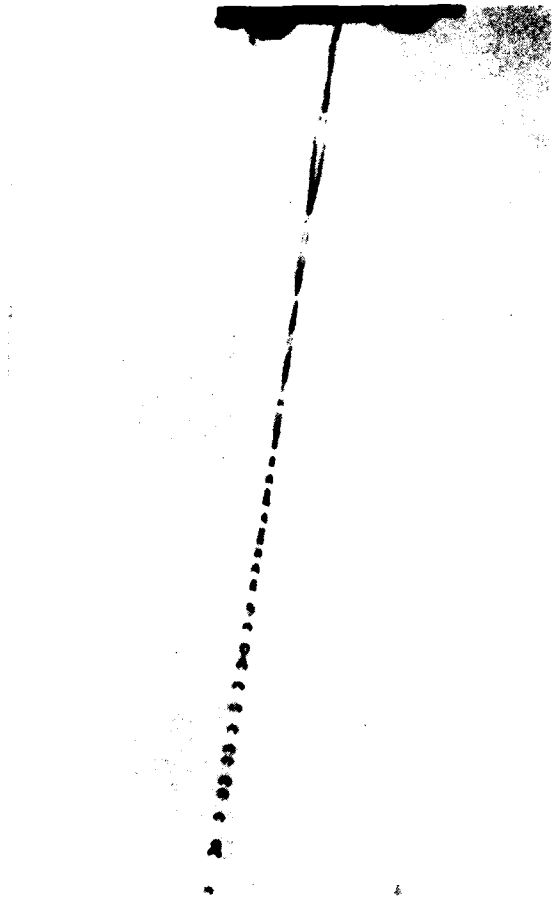

Figure 33. Sheet of Fluid Emerging from a Slot with an Offset Entrance Hole, 10 cps Fluid

This experiment shows that the bimetal nozzle process can be used to make nozzles that form jets whose trajectories can be controlled. A jet can be deflected from a path perpendicular to the nozzle plate and the deflection angle is controlled by the misalignment of the two electroformed holes which form a nozzle.

From one flat nozzle plate, an array of diverging or converging jets can be formed. Diverging jets improve the mixing of the droplets and the air. The impact of converging jets can improve the liquid atomization.

5.4.2 Stable Fluid Sheet with Swirl and Expansion

The sheet formed by a rectangular nozzle plate with a swirl entrance slot is shown in Figure 34. The sheet rotates and widens due to the swirl built into the nozzle. It eventually transforms into four round jets and these round jets break into drops due to the capillary instability. This photograph clearly shows the basic stability of a sheet of fluid. The smoothness of this sheet is a result of the laminar flow created by the bimetal nozzles.

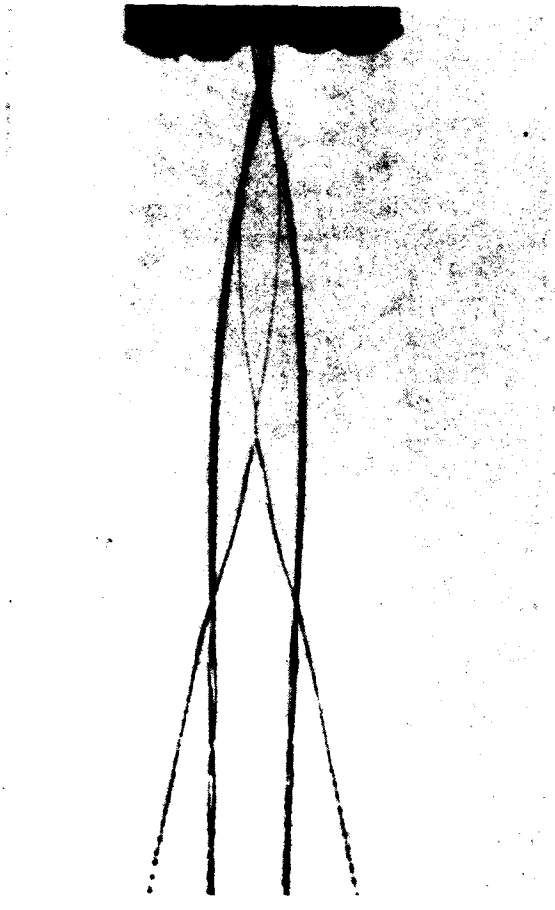

Figure 34. A Twisting Sheet Formed at a Rectangular Nozzle with a Rotated Entrance Slot

5.4.3 Varicose Instabilities on a Fluid Sheet from a Complex Nozzle

Figure 35 shows ligaments being formed after an acoustic drive is applied to the sheet shown in Figure 34. This photograph demonstrates a benefit of the complex nozzle structure. These ligaments are expanding lengthwise after they separate from the sheet. The ligaments break into drops and the drops spread apart after formation. This complex nozzle structure thus produces a flow pattern in the sheet that prevents agglomeration and the atomization is preserved.

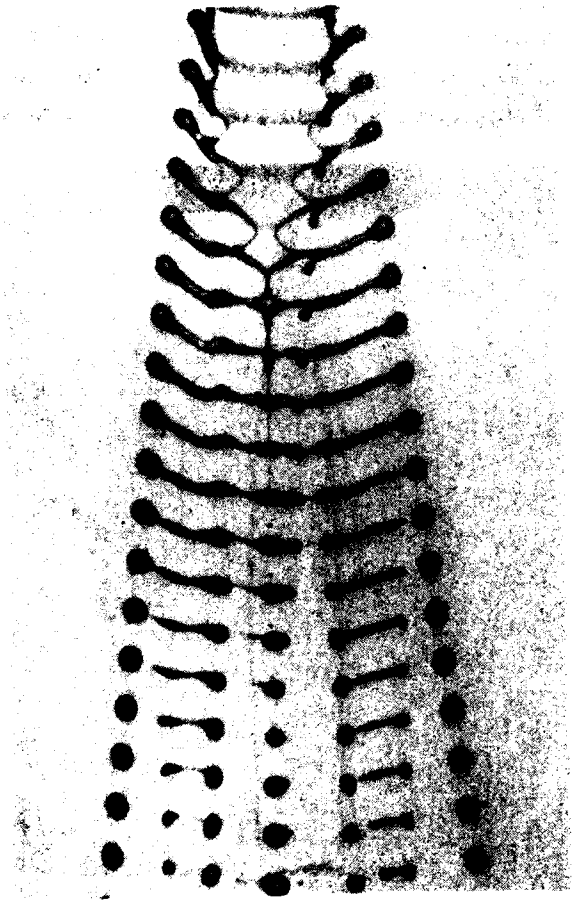

Figure 35. A Sheet from a Nozzle with Swirl, Breaking into Ligaments and Drops Due to High-Power Acoustic Drive, 10 cps Fluid

This photograph can be compared to the one in Figure 29 which shows ligaments being formed from a nozzle with a simple structure. In Figure 29, the drops have a velocity that moves them to the center of the flow. The drops are moving from top to bottom in the photograph and they are shown moving together as they move away from the nozzle. Out of the view of this photograph, the drops eventually coalesce into a larger drop, destroying part of the atomization.

Figure 36 is another example of the ligaments that can be made from the sheet of Figure 34. As the ligaments move from the top of the photograph to the bottom, the varicose perturbations grow and the ligament breaks into drops. Since the acoustic drive is periodic and the process is extremely repetitive, this photograph can be looked upon as a history of the varicose instabilities on a filament.

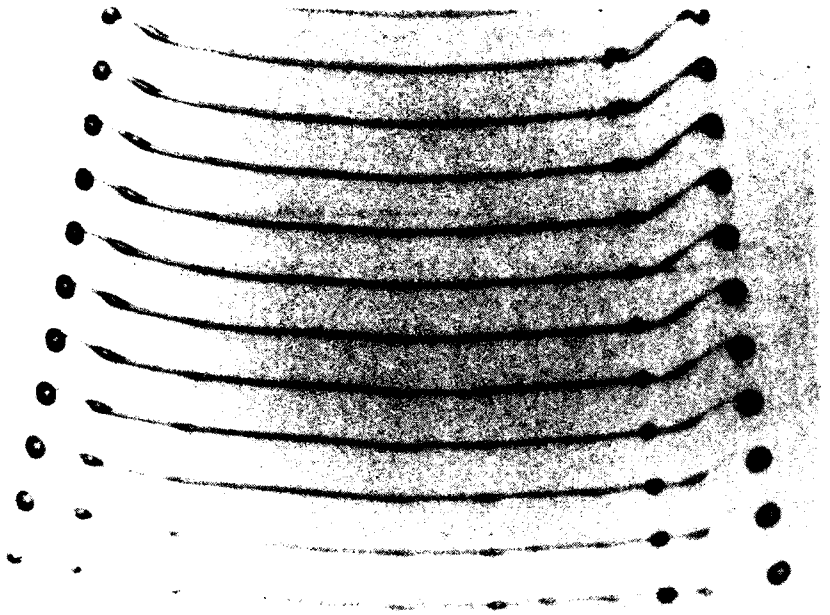

Figure 36. Tubes, Formed at 16.8 kHz from a Sheet Formed by a Complex Nozzle, Breaking into Drops, 10 cps Fluid.

5.4.4 Stable Fluid Sheet with Notches, Swirl and Expansion

The nozzle plate with width perturbations and with a swirl entrance slot, shown in Figure 16, was operated with the 10 cps fluid and with no acoustic drive. The photograph in Figure 37 shows the twisting sheet that formed. This photograph can be compared to Figure 34 which shows a sheet from a complex rectangular nozzle without notches. The difference between the two sheets is that the sheet from the notched rectangular slot, Figure 37, is not as steady as the sheet from the rectangular nozzle, Figure 34. The notches or spatial perturbations produce some turbulence in the sheet and this turbulence makes an unsteadiness in the sheet.

5.4.5 Loop and Drop Formation on a Fluid Sheet from a Notched Complex Nozzle

The nozzle plate with width perturbations and with a swirl entrance slot, shown in Figure 16, was operated with the 10 cps fluid and an acoustic drive at 11.2 kHz. The photograph in Figure 38 shows the evolution of a perturbation created by one of the notches on the side of this fluid sheet.

The initial disturbance takes the form of a loop structure that rises out of the side of the sheet. The perimeter of the loop is thick and there is a thin layer of liquid across interior of the loop. Sometimes the thin layer across the center of the loop could be made to puncture and the interior of the loop would be open. It was difficult to adjust

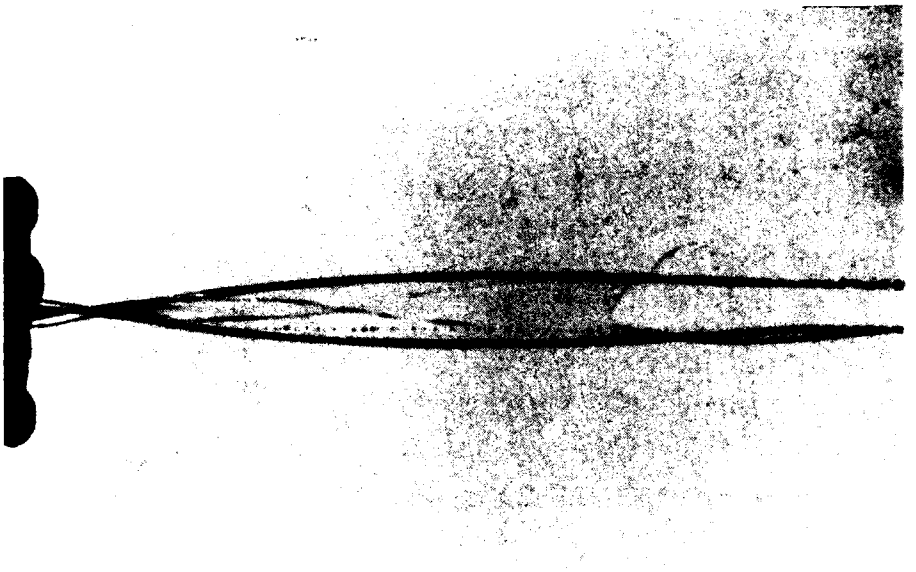

Figure 37. A Twisting Sheet Formed at a Notched Rectangular Nozzle with a Rotated Entrance Slot, 10 cps Fluid

the power and frequency to achieve these open loops and no photographs were obtained of this phenomena.

As the sheet moves, the loop extends from the sheet and becomes more oval shaped. The two opposite edges of the loop merge, forming a ligament extending from the side of the sheet. The ligament ejects a drop from its end and then collapses back to the sheet.

Depending on the amplitude of the acoustic driving signal, the ligament responded in several ways. It could eject a drop from its end and then collapse back to the sheet, as shown in Figure 38. The ligament could also disconnect from the sheet and then break into a series of drops by ligament breakup mechanisms. If the acoustic drive was not large enough, it would collapse back into the sheet with no drop production.

Figure 38 can be compared to Figures 35 and 36. In the earlier photographs, the nozzle contained no spatial perturbations (notches) and the breakup produced ligaments that travelled along the trajectory of the original sheet. This atomization process did not spread the sheet of ligaments perpendicular to the trajectory of the undriven sheet.

When the spatial perturbations are built into the nozzle, the added turbulence produces a small effect on the undriven sheet.

When the spatial perturbations are combined with temporal perturbations (the acoustic drive), the effect on the atomization is striking. Figure 38 shows that driving the sheet with both spatial and temporal perturbations creates a sheet of drops which ejects drops from its spatial. The spatial distribution of the spray can be varied over a wide range by varying the power in the acoustic drive.

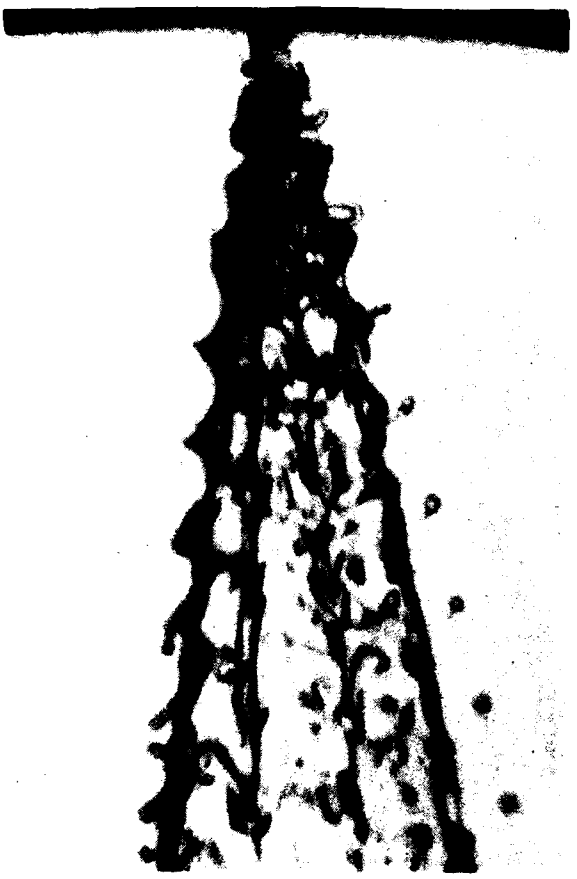

Figure 38. Loops Form Ligaments that Eject Drops, 11.2 kHz

5.4.6 Spray Formation from a Fluid Sheet Formed at a Notched Complex Nozzle

The same nozzle plate used to obtain Figures 37 and 38 was used to examine the feasibility of using the drop generator with a complex nozzle as a throttle body fuel injector in an automobile engine. It was operated at a high acoustic-power level so that a simulated useable fuel spray was formed. The spray is shown in Figure 39.

At the operating pressure, this nozzle produced a flow of 15 litres per hour. This flow rate is approximately what an automobile engine requires.

This test required 13 watts of power for the piezoelectric driver. If this sprayer was used in an automobile, it would probably use from 25 to 50 watts of power from the engine alternator. This is a practical load for the alternator.

The 10 cps fluid was used to demonstrate the atomization of thicker liquids. More viscous liquids are desirable for fuels because they are less volatile and produce less pollution from evaporation.

The photograph shows that the produced spray did not have a dense region in the

Figure 39. Spray is Created from a Notched Rectangular Nozzle With a Rotated Entrance Slot, 13 watts, 5.55 kHz.

center. Sprays from square and circular nozzles tend to have a dense spray in the center and that is shown in Figures 45 and 46(which appear in Sections 5.5.4 and 5.5.5). The complex rectangular nozzle has spread the fluid over a wide region and there does not seem to be a concentration of fluid at any particular spot.

This complex nozzle creates a fan spray that diverges away from the nozzle. This divergence eliminates the dense edges of the spray, which occur with the simple rectangular nozzle shown in Figure 28.

The notches in the nozzle produce streams of larger drops in the spray pattern and these are distributed over the width of the spray. There are small drops spread throughout the extent of the spray and the photograph shows these drops to be uniformly distributed.

This test shows that the drop-generator design is a feasible fuel sprayer for internal combustion engines. The spray is uniformly distributed and that makes it possible for a uniform fuel charge to be distributed to the separate cylinders from one source.

5.5 Experiments on Commercial Nozzles

5.5.1 Liquid Cone Nozzles

The photographs of the atomized jet in Figures 25 and 26 show that there is a region of large drops in the center of the spray pattern. To modify the spatial distribution of the spray, we added swirl to the injector manifold. With this added swirl, a hollow cone of liquid is produced from the circular nozzle. The nozzle plate used for this experiment is a 700-micron diameter hole and it is made from the same artwork as the 750-micron plate used in Figure 25.

Figure 40 shows the cone after an acoustic drive was applied. The excitation forces the cone to break into rings of liquid which then disintegrate into drops. The spray pattern formed is thus hollow.

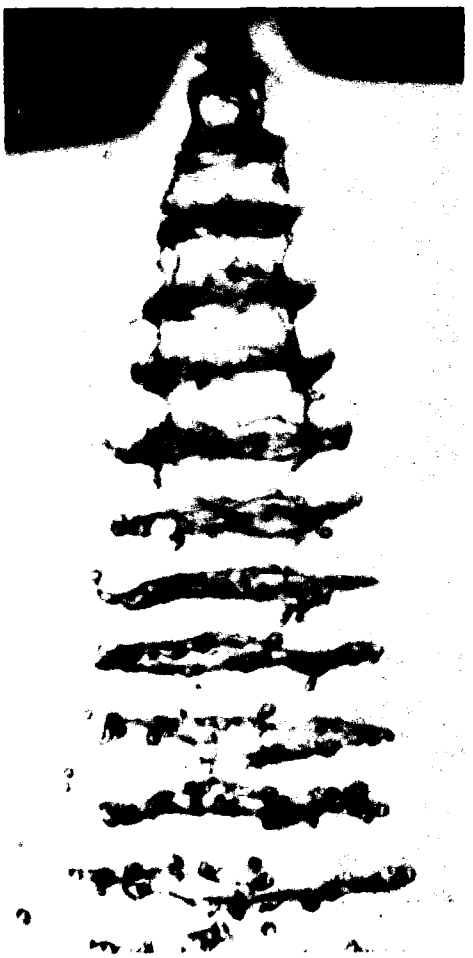

Figure 40. A Jet with Swirl Diverges into a Cone that is Broken into Rings by the Acoustic Drive, 23.8 kHz

This example demonstrates that the addition of swirl in the manifold eliminates the dense spray along the jet axis.

5.5.2 Simplex Nozzle

A simplex nozzle is a basic nozzle design used for producing cone sprays. The nozzle produces turbulence in the fluid and this turbulence helps to drive the atomization. Unlike the sheet-forming bimetal nozzles we have tested, the simplex nozzle will atomize the fluid without any acoustic drive.

We replaced the nozzle plate on the end of the piezoelectric driver with a simplex nozzle and tested the simplex nozzle with acoustic assist. We call this acoustic assist because it assists and modifies the atomization.

A photograph of the simplex nozzle in operation with no acoustic drive is shown in Figure 41. The nozzle forms a cone shaped sheet which eventually atomizes. The cone is

Figure 41. A Simplex Nozzle with No Acoustic Assist

affected by the Kelvin-Helmholtz instability. This instability causes the sheet to flap and this flapping makes the spray spatially nonuniform. The drops tend to be concentrated in packets and the fluid density is much higher in the packet than in the surrounding area.

Several packets of drops are visible on the right side of Figure 41.

By applying the acoustic signal to the fluid cone, we can have a large effect on the spray produced by the simplex nozzle.

In earlier experiments on cylindrical jets, we used a low-power acoustic drive to establish initial conditions for the existing Rayleigh instability. We also applied large velocity perturbations to the jet and created a new type of instability.

The same approach can be used here to establish initial conditions for the Kelvin-Helmholtz instability and to also create new instabilities on the fluid cone.

Figure 42 is a photograph of the simplex nozzle with an acoustic assist at 6.8 kHz. The acoustic drive produces ring-shaped disturbances on the cone. Ligaments form on this ring, extending both into the interior of the cone and radially outward.

Figure 42. A Simplex Nozzle with Acoustic Assist at 6.8 kHz

The perturbations established by the acoustic signal will establish initial conditions for the Kelvin-Helmholtz instability. By setting the frequency for the Kelvin-Helmholtz instability at a high level, the wavelength between clusters of fluid will be decreased and the volume of fluid in each cluster will be decreased. This should result in a more spatially uniform spray.

The high-amplitude velocity perturbations also create ligaments that emerge from the sides of the cone. These ligaments create drops and widen the spatial distribution of the spray.

The driven spray shown in photograph Figure 42 looks more uniform than the undriven spray in Figure 41. However, there is no quantitative data at this time to show conclusively that the spray uniformity has been improved.

5.5.3 Square Hole Nozzle

A nozzle from an automobile fuel injector was provided by Ford Motor Car Company. This nozzle was made of silicon metal and the hole was etched into the metal using photofabrication techniques. This process is described by Bassous[50] and it makes square, tapered holes in the silicon.

Figures 30 and 38 showed that spatial thickness perturbations along with large temporal velocity perturbations create ligaments that extend from the surface of a flat fluid sheet. This experiment with a square nozzle was conducted to determine if the same technique of placing perturbations in a nozzle periphery can be used to extend fluid ligaments from a round jet.

Here, we consider each corner of the square nozzle to be a spatial perturbation on the edge of a round jet. With no acoustic drive, the jet emerging from the square hole simply goes to a round shape and then breaks into drops by Rayleigh breakup. When the acoustic drive is applied, the jet is atomized with a spatial density distribution defined by the nozzle shape. There are four ligaments of fluid extending radially from the core of the jet, one for each corner or perturbation on the nozzle.

A photograph of the atomization produced by applying an acoustic drive to the square nozzle is shown in Figure 43. Ligaments, arranged in layers of four, extend from the jet and break into drops by Rayleigh breakup.

Figure 43 can be compared to Figures 26 and 27 which show photographs of round jets excited with only temporal velocity perturbations. When only temporal perturbations were used with a round jet, the jet was atomized and the spatial distribution of the spray was random. Comparing Figures 26 and 27 shows the significant change made in the spatial distribution of the spray by placing spatial perturbations on the round nozzle to make it square.

Figure 43. Spray Formation from A Square Silicon Hole Driven at 27.9 kHz

5.5.4 Cross-Shaped Nozzle

The cross-shaped nozzle, earlier shown in Figure 18, was fastened to the acoustic driver and the resulting spray was photographed at several frequencies. This experiment is another example that use of both spatial and temporal drive creates drops that are ejected perpendicular to the initial trajectory. The result is a cone-shaped spray and the cone angle is a function of the amplitude of the acoustic drive.

Figure 44 shows that at 7.7 kHz the jet is atomized by a process that first forms discs and then the discs break into drops. The spray seems to be more uniform in the azimuthal direction than one would expect from the shape of the nozzle.

In Figure 45 at a drive frequency of 21.3 kHz, ligaments extend radially from the jet and these ligaments break into drops. At this frequency, a large portion of the liquid remains along the axis of the undriven jet. The spray that forms has a pattern that is four-sided like the cross-shaped nozzle.

Figure 44. Jet from Cross-Shaped Hole. Driven at 7.7 kHz

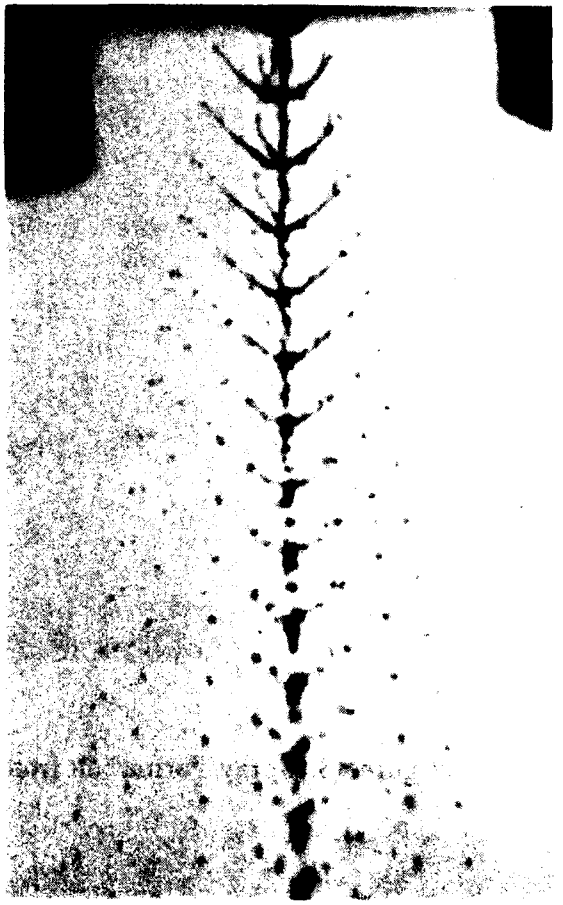

Figure 45. Jet from Cross-Shaped Hole, Driven at 21.3 kHz

This nozzle shape does not appear to be as effective as the square nozzle in ejecting the spray radially. Figure 43 shows that the spray from the square nozzle leaves a smaller

volume of fluid along the axis of the jet than the cross-shaped nozzle.

5.5.5 Large Drilled Round Nozzle

A typical diameter for a nozzle in a rocket engine is 0.090 inch. We conducted a test to determine if the the high-power acoustic drive could atomize a jet of this diameter. This particular test was conducted at a flow rate of 30 gallons/hour.

Figure 46 is a photograph of the nozzle operating at 30 gallons/hour. It shows that most of the mass in the initial stream is atomized. A dense core does however remain along the initial jet axis.

Figure 46. A 30 Gallon per Hour Spray from the 2-Inch-Diameter Acoustic Driver, Driven at 7.2 kHz

In a typical rocket engine, there is gas flowing along the fluid jet. The atomization produced by the acoustic signal would drive a major portion of the liquid radially from the jet into the gas stream. For this situation of a jet with coflowing gas, the acoustic drive would greatly enhance the mixing of the gas and liquid.

6 Proposed Additional Work

6.1 Combustor Instabilities

The driving mechanism for the atomization of fuel in turbine engine combustors is the Kelvin-Helmholtz instability. The fuel is introduced into the combustor along with a stream of air. The difference in velocities of the fuel and air flows drives this instability. Wind-driven waves and the flapping of a flag in the breeze are examples of a Kelvin-Helmholtz instability.

In a turbine engine combustor, the fuel spray is usually not uniformly distributed in either space or time. The fuel drops collect in regions that are called clusters. The burning of these clusters produces large temperature variations in the combustor and these nonuniformities can be the source of two combustion problems: noise and pollution.

Noise is a problem for several reasons. The noise-driven flexing of the combustor can induce metal fatigue and result in cracking of the combustor components. The noise is also objectionable; it must be muffled because it annoys nearby people.

The temperature variations that contribute to noise can also create pollution. The hot spots in the flame can create nitrous oxide pollution. The cold spots retard the combustion rate, requiring that the combustor be longer than necessary to assure that all the fuel is burned before the combustion mixture exits the combustor.

One possible source of the uneven spray, in both space and time, is the amplification of the low-frequency noise by the Kelvin-Helmholtz instabilities on the continuous liquid sheet. This instability is convective. That is, it grows in space with respect to an observer sitting on the combustor. These spatial variations in the fuel spray cause uneven pressure and temperature fluctuations throughout the combustor. These pressure fluctuations are fed back to the fuel-injector nozzle through the combustor structure and vibrate the injector. The injector vibrations establish the initial conditions for the Kelvin-Helmholtz instability which leads to the formation of fuel clusters.

The combustor and fuel injector can possibly become a feedback system, with the pressure variations from the fuel density nonuniformities creating the fuel-injector vibrations that contribute to fuel density nonuniformities. The combustor instabilities made by this proposed mechanism are mathematically similar to the instabilities used in the first travelling-wave amplifier for audio signals. This amplifier used the varicose or sausage instability on a liquid jet and it was built by Chichester Bell, a cousin of Alexander Graham Bell, and described by Boys [51].

6.2 Combined Acoustic and Air Blast Atomization

In the project work done up until now, the fluid has been atomized by a velocity perturbation placed in the fluid sheet. This velocity perturbation has been created by piezoelectric drivers or by turbulence that was created by the nozzle. We have used various nozzle and acoustic driver configurations and produced atomization that has been the result of either turbulence or acoustic drive acting alone, or the result of a combination of acoustic drive and nozzle created turbulence.

During Phase II of this contract, we discovered that we could easily atomize fluid

sheets by means of amplitude dependent instabilities. This atomization mechanism has been largely ignored because previously there was no method to generate the necessary acoustic signal.

For a follow-on project, we propose to add an air flow to the drop generator so that the atomization will be the result of velocity perturbations and the Kelvin-Helmholtz instability.

We can affect the atomization in two ways. The first is by using the acoustic signal to establish the initial conditions for the Kelvin-Helmholtz instability. The second is by driving fluid-air instabilities that presently do not exist in the combustors.

By acoustically driving the Kelvin-Helmholtz instability, we can possibly decrease the magnitude of the present instabilities in the combustor. If the fuel injector is driven with a large amplitude signal, the length of the continuous fluid sheet would be reduced and the amplification of noise in the combustor by the travelling-wave amplifier made by the fluid sheet would also be reduced. This driving signal would be at a higher frequency than the combustor resonances so its perturbations would not add to the noise.

The fluid sheet length can be further reduced by acoustically driving additional instabilities. The thickness mode instability, shown in Figure 40 is one that probably can not occur without our acoustic driver. The acoustic frequency used to drive the thickness instability can be selected so that it does not match any resonances of the combustor structure. Driving additional instabilities in the combustor may also produce additional clusters. If the number of fuel clusters is increased, the amount of fuel in each cluster should decrease.

The result of this follow-on project could be a more uniform fuel spray that will lead to more uniform combustion. The benefit will be a uniform flame temperature that results in less pollution and less noise.

The proposed drop generator is shown in Figure 47. The fluid flow originates in the acoustic driver and flows through a tube surrounded by an air or gas chamber. The fluid and air are ejected from the end of the device. The fluid tube can have various nozzles placed in its end or the tube can be used without an additional nozzle. The diameter of the fluid tube can be changed. Both the air and fluid flows can be controlled and the acoustic drive can be varied in frequency and amplitude.

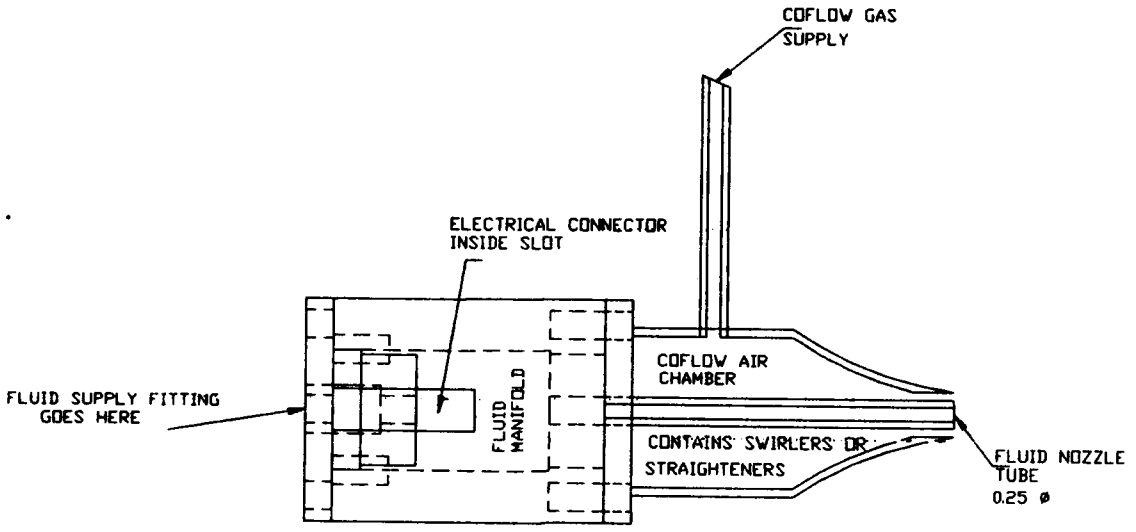

Figure 47. Proposed Drop Generator Combining Air Flow with Acoustic Drive.

7 References

[1] S. Chandrasekhar. *Hydrodynamic and Hydromagnetic Stability.* Oxford University Press at the Clarendon Press, Ely House, London W.I., 1961.

[2] Adel Mansour and Norman Chigier. Dynamic behavior of liquid sheets. *Physics of Fluids A*, 3(12):2971–2980, Dec 1991.

[3] Adel Mansour and Norman Chigier. Disintegration of liquid sheets. *Physics of Fluids A*, 2(5):706–719, May 1990.

[4] H. B. Squire. Investigation of the instability of a moving liquid film. *British Journal of Applied Physics*, 4:167–169. Jun 1953.

[5] G. D. Crapper, N. Dombrowski, W. P. Jepson, and G. A. D. Pyott. A note on the growth of Kelvin-Helmholtz waves on thin liquid sheets. *Journal of Fluid Mechanics*, 57(4):671–672, 1973.

[6] G. D. Crapper, Norman Dombrowski, and G. A. D. Pyott. Large amplitude kelvin-helmholtz waves on thin liquid sheets. *Proceedings of the Royal Society, London*, A(342):209–224, 1975.

[7] R. H. Rangel and W. A. Sirignano. The linear and nonlinear shear instability of a fluid sheet. *Physics of Fluids A*, 3(10):2392–2400, Oct 1991.

[8] W. W. Hagerty and J. F. Shea. A study of the stability of plane fluid sheets. *Journal of Applied Mechanics*, 22:509–514, Dec 1955.

[9] J. W. S. Rayleigh. On the instability of jets. *Proc. London Math. Society*, 10:4, 14-Nov 1878.

[10] D. J. Ryley and M. R. Wood. The construction and operating characteristics of a new vibrating capillary atomizer. *Review of Scientific Instruments*, 40:303–305, 1963.

[11] B. J. Mason and J. L. Brownscombe. Production of uniform size drops at controllable frequency and spacing from a vibrating capillary. *Journal of Scientific Instruments*, 41:258, 1964.

[12] N. R. Lindblad and J. M. Schneider. Production of uniform-sized liquid droplets. *Journal of Scientific Instruments*, 42:635–638, 1965.

[13] E. K. Dabora. Production of uniform sprays. *The Review of Scientific Instruments*, 38(4):502–506, Apr 1967.

[14] John L. Dressler and Gilbert O. Kraemer. A multiple drop-size drop generator for calibration of a phase-doppler particle analyzer. In *Liquid Particle Size Measurement Techniques:Second Volume,ASTM STP 1083*, E. Dan Hirleman, W.D. Bachalo, and Phillip g. Felton, editors, pages 30–44, 1916 Race St., Philadelphia PA 19103, Aug 1990. American Society for Testing and Materials, ASTM.

[15] E. A. Ibram and A. J. Przekwas. Impinging jet atomization. *Physics of Fluids A*, 3(12):2981-2987, Dec 1991.

[16] John Zeleny. Instability of electrified liquid surfaces. *The Physical Review, Second Series*, 10(1):1-6, Jul 1917.

[17] R. H. Magarvey and L. E. Outhouse. Note on the break-up of a charged liquid jet. *Journal of Fluid Mechanics*, 13(Part 1):151-157, May 1962.

[18] A. L. Huebner. Disintegration of charged liquid jets. *Journal of Fluid Mechanics*, 38(4):679-688, 1969.

[19] A. H. Lefebvre, X. F. Wang, and C. A. Martin. Spray characteristics of aerated-liquid pressure atomizers. *J. Propulsion*, 4(4):293-298, Jul 1988.

[20] J. M. Crowley. Growth and excitation of electrohydrodynamic surface waves. *Phys. Fluids*, 8(9):1668-1676, Sep 1965.

[21] David J. Rose and Jr. Melville Clark. *Plasmas and Controlled Fusion.* The M.I.T. Press, Massachusetts Institute of Technology, Cambridge, Massachusetts, Feb 1961. Chap. 14, Chap. 15.

[22] F. D. Ketterer and J. R. Melcher. Electromechanical costreaming and counter streaming instabilities. *Physics of Fluids*, 11(10):2179-2191, Oct 1968.

[23] J. R. Melcher. Complex waves. *IEEE Spectrum*, pages 86-101, Oct 1968.

[24] James R. Melcher and E. Paul Warren. Continuum feedback control of a rayleigh-taylor type instability. *The Physics of Fluids*, 9(11):2085-2094, Nov 1966.

[25] Joseph M. Crowley. Stabilization of a spatially growing wave by feedback. *The Physics of Fluids*, 10(6):1170-117, Jun 1967.

[26] John L. Dressler. Videotype sampling in the feedback stabilization of electromechanical equilibria. In *Feedback and Dynamic Control of Plasmas*, T.K. Chu and H.W. Hendel, editors, pages 60-67, New York, Jun 1970. American Institute of Physics.

[27] Brian Dunne and Benedict Cassen. Some phenomena associated with supersonic jets. *Journal of Applied Physics*, 25(5):569-572, May 1954.

[28] Brian Dunne and Benedict Cassen. Velocity discontinuity instability of a liquid jet. *Journal of Applied Physics*, 27(6):577-582, Jun 1954.

[29] P. D. McCormack, L. Crane, and S. Birch. An experimental and theoretical analysis of cylindrical liquid jets subjected to vibration. *Britt. J. Appl. Phys.*, 16(3):395-408, Mar 1965.

[30] L. Crane, S. Birch, and P. D. McCormack. The effect of mechanical vibration on the break-up of a cylindrical water jet in air. *Britt. J. Appl. Phys.*, 15(6):743-751, Jun 1964.

[31] Milton Van Dyke. *An Album of Fluid Motion*, volume 0-91576-03-7. The Parabolic Press, P.O. Box 3032, Stanford CA, 1982. Photograph 149, page 87.

[32] J. L. Dressler. Shock model of liquid jet breakup. Technical Report UCRL-78480-Rev. 1, Lawrence Livermore National Laboratory, Oct 1976.

[33] Richard W. Sellens. Prediction of the drop size and velocity distribution in a spray, based on the maximum entropy formalism. *Part. Part. Syst. Charact.*, 6:17–27, 1989.

[34] L. P. Chin, P. G. LaRose, R. S. Tankin, T. Jackson, J. Stutrud, and G. Switzer. Droplet distributions from the breakup of a cylindrical liquid jet. *Physics of Fluids A*, 3(8):1897–1906, Aug 1991.

[35] Richard G. Sweet. High frequency recording with electrostatically deflected ink jets. *Review of Scientific Instruments*, 36(2):131–136, Feb 1965.

[36] R. W. Park and E. J. Crosby. A device for producing controlled collisions between pairs of drops. *Journal of Chemical Engineering Science*, 20:39–45, 1965.

[37] Richard H. Lyon and John A. Robertson. Apparatus and method for generation of drops using bending waves. U.S. Patent (3,793,393), 12 Jun 1973.

[38] Charles Cha, George W. Denlinger, David N. Pipkorn, and Elias Spyrou. Jet drop printer with elements balanced about support plate in nodal plane. U.S. Patent (4,198,643), 15 Apr 1980.

[39] W. R. Beaudet. Fluid jet print head having resonant cavity. U.S. Patent (4,587,528), 6 May 1986.

[40] Allen Rosencwaig, Jackson C. Koo, and John L. Dressler. Method for producing small hollow spheres. U.S. Patent (4,257,799), Mar 24 1981.

[41] Harvey L. Berger, Earle Ericson, and Carl Levine. Ultrasonic liquid atomizer, particularly for high volume flow rates. U. S. Patent (4,541,564), 17 Sep 1985.

[42] Masami Endo, Kakuro Kokubo, Yoshinobu Nakamura, and Daijiro Hosogai. Vibrating element for use on an ultrasonic injection nozzle. U. S. Patent (4,756,478), 12 Jul 1988.

[43] Rodger L. Gamblin. Orifice plate construction. U.S. Patent (4,528,070), 9 Jul 1985.

[44] David B. Wallace, Donald J. Hayes, and J. Michael Bush. Study of orifice fabrication technologies for the liquid droplet radiator. NASA Contractor Report 187114, NASA Lewis Research Center, Cleveland OH 44135, May 1991. Contractor: MicroFab Technologies, Inc.; Contract NAS3-25275.

[45] Reinhard Glang and Lawrence V. Gregor. Generation of patterns in thin films. In *Handbook of Thin Film Technology*, Leon I. Maissel and Reinhard Glang, editors, pages 7.1–7.66, New York, 1970 McGraw-Hill.

[46] W.A. Strauss Jr. Applications of photo-etching in the manufacture, interconnection and packaging of micro-circuits. *SCP and Solid State Technology*, 9(2):15–18, Feb 1966.

[47] R. P. Fraser, Norman Dombrowski, and Paul Eisenklam. Vibrations as a cause of disintegration in liquid sheets. *Nature*, 173(4402):495, 13 Mar 1954.

[48] P. H. Schweitzer. Mechanism of disintegration of liquid jets. *Journal of Applied Physics*, 8:513–521, Aug 1937.

[49] J. L. Dressler and T. A. Jackson. Acoustically driven liquid sheet breakup. In *ILASS-Americas 4th Annual Conference*, volume 4, pages 137–141, Hartford CT, May 1990.

[50] Ernest Bassous. Nozzles formed in monocrystalline silicon. U. S. Patent (3,921,916), 25 Nov 1975.

[51] C. V. Boys. *Soap Bubbles, Their Colors and the Forces Which Mold Them.* Dover Publications Inc., 180 Varick Street, New York, NY, 1 edition, 1959.

Appendix A Fluid Solutions

A.1 Fluid Properties and Ingredients

The operational test fluids were made to have the following properties:

1. Noncorrosive
2. High-Surface Tension, 60+ dynes/cm2
3. Sterile - Do not support microbe growth
4. NonDrying
5. Viscosity of 1 to 10 cP

The required properties for the operational test fluid are also the desired properties for the inks used in continuous-jet ink jet printers. The requirements for ink jet printing fluids are met by mixing six components, one of which is dye. After eliminating the dye, the following list of five components will form the basis of the fluids that were used for this project:

1. Solvent
2. Humectant
3. Buffer
4. Antimicrobial Agent or Preservative
5. Corrosion Inhibitor(s)

The solvent used for operational test fluid is water. It has a high-surface tension, low viscosity, and is not a fire or vapor hazard.

The inclusion of the humectant is not essential for the operation of the droplet generator but it makes the startup of the drop generator easier. The important characteristics of a humectant are that it does not dry and it dissolves readily in water. When the drop generator is turned off and drained of fluid, some of the fluid remains in the manifold and in the nozzles. After the water evaporates from this fluid, a layer of the humectant remains, coating the fluid chambers and the nozzles. The buffer and preservative will be held in this humectant layer. When the unit is restarted, the fluid quickly mixes with the humectant and the chemicals in the humectant are quickly dispersed and dissolved into the operational test fluid. If the humectant were not included in the fluid, the buffer and preservative would form deposits in the manifold and nozzles when the water evaporated. When the drop generator was restarted, the jets would form erratically due to these deposits. Eventually, even without the humectant, the deposits of dried buffer and preservative will redissolve in the fluid and the jets will form properly. Commonly used humectants are ethylene glycol, diethylene glycol, and glycerol.

The buffer is a necessary ingredient to prevent corrosion of the nickel nozzle plates. Since distilled water has a very unstable pH, it can become acidic and dissolve the nickel that forms the nozzle. By buffering the water, the pH can be held near the neutral value and the nickel will not be corroded.

The corrosion inhibitor is needed because the nozzle plates are made from laminations of two different metals and the presence of the fluid causes galvanic corrosion to occur between them. The copper layer in the nozzle-plate center will be dissolved into the fluid and the strength of the nozzle plate will be destroyed. The problem is identical to the corrosion of an automobile copper radiator due to the presence of the iron engine block. Several commercial products are available for preventing corrosion in automotive cooling systems and these products work for nozzle plates also. Two common corrosion inhibitors are benzotriazole and tolytriazole. These are commodity chemicals and they are available from several vendors, under various trade names. An additional corrosion inhibitor is added to prevent galvanic corrosion that may occur between the metals in the plate and any stainless steel that may be present in the fittings and tank. Suitable materials, also used in preventing corrosion in automobile cooling systems, include sodium nitrite and/or sodium molybdate which pacifies the stainless steel by forming an oxide layer. Sodium nitrite is also a commodity chemical and is readily available. Sodium molybdate is available from Climax Molybdenum or a laboratory supply house.

The preservative is required because the buffer, humectant, and corrosion inhibitor may support microbe growth. If microbes grow in the fluid, the filters in the fluid system will be quickly plugged. The antimicrobial agent must be water soluble, broad spectrum in its activity, and stable at neutral and slightly basic pH conditions. An inexpensive and available preservative, that is also used in textile printing, is formaldehyde. The problem with formaldehyde is that it is volatile and slowly evaporates from the fluid. The life of the preservative in the operational test fluid is therefore limited. The odor is also offensive. Longer lasting preservatives, that also meet the other criteria and are used in both printing inks and textile dyes, are Giv-Gard DXN (available from Givaudan Corp.) and Dowicil 75 (available from Dow Chemical Company).

The chemical used to change the fluid viscosity is glycerol. This is a commodity chemical that has good experimental properties. It also acts as the humectant. It is miscible with water in any quantity and its surface tension is close to that of water. When making experimental drop fluids of glycerol and water, the viscosity will vary with the proportion of glycerol but the surface tension will remain almost constant.

A.2 Standard Water-Like Operational Test Fluid

A.2.1 Chemical Formula

Percentages are on a weight/weight basis

1.	Ethylene glycol	1.0%
2.	Give-Gard DXN	0.1% *
3.	Borax (sodium borate decahydrate)	0.1%
4.	Sodium Nitrite	0.1%

5.	Benzotriazole	0.01%
6.	H_2O (distilled)	Balance
7.	Conc. NaOH for final pH adjustment. (I use 33 percent w/w. Under 10 mls are required for adjustment.)	

*Note: Give-Gard DXN is supplied as a 92 percent solution. When it is dissolved in water, it hydrolyzes forming acetic acid as a by-product. I prefer to hydrolyze the Giv-Gard prior to adding it to the fluid so that the pH of the fluid is stable more quickly. I therefore prepare a 20 percent aqueous solution as a stock solution, allowing it to completely hydrolyze prior to use. (This takes several hours.)

A.2.2 Mixing Procedure

1. Fill a mixing container with about 90 percent of the distilled water you will need depending on batch size.

2. Add the ingredients one thru five, in order, with mixing in between.

3. Mix for about 30 minutes to completely dissolve all the solid components.

4. Adjust the pH to about 8.1 with 33 percent NaOH.

5. Add the remaining water to bring it to batch size. Mix thoroughly and allow to set to equilibrate for about an hour.

6. Remix for about 10 minutes and recheck pH. Readjust if necessary (NaOH to increase or acetic acid to decrease). Rarely is this adjustment necessary. The pH is stable.

A.3 High-Viscosity Operational Test Fluid (10 cps)

A.3.1 Chemical Formula

Percentages are on a weight/weight basis.

1.	Glycerol	60.0%
2.	Giv-Gard DXN	0.1%
3.	Borax (sodium borate decahydrate)	0.2%
4.	Sodium Nitrite	0.1%
5.	Benzotriazole	0.01%
6.	H_2O (distilled)	Balance
7.	Conc. NaOH for final pH adjustment	

A.3.2 Mixing Procedure

The mixing procedure is the same as for the water-like fluid above. More borax is used here than in the water-like fluid because the high level of glycerol lowers the unadjusted pH of this fluid.

Appendix B List Of Drop Generator Component Vendors

1. Bellofram Corporation, 30 Blanchard Road, Burlington MA 01803
   Telephone 800–225-1031 or 617-272-2100
   Manufacturer of gas pressure regulator for fluid supply
   Mfg. of 10-inch Cartridge Filters and Housings

2. Allied Valve Industries, Inc., 1019 West Grand Avenue
   Chicago IL 60622-6590
   Telephone 312-226-1506
   Supplier of pressure relief valve for fluid supply
   Valve manufactured by Kunkle Valve Co.
   Kunkle Pressure Relief Valve PN 48A-100psi

3. EIL Instruments, Inc.,
   96A Westpark Drive, Dayton OH 45459
   Telephone 513-435-2134
   Manufacture of digital pressure readout
   EIL Process Controller Model AN240-0-1-0-A

4. Omega Engineering, P.O. Box 4047
   One Omega Drive, Stamford CT 06907
   Telephone 203-359-1660 or 800-826-6342
   Supplier of Model 102 Pressure Sensor for Manifold Pressure

5. Tanyx Measurements, Inc., 505 Middlesex TurnPike
   Billerica MA 01821
   Telephone 508-671-0183
   Alternate Supplier of AB-25 Pressure Sensor

6. Alloy Products Corp., P.O. Box 529, 1045 Perkins Avenue
   Waukesha WI 53187-0529
   Telephone 414-542-6603
   Mfg of 5 gal. stainless steel pressure tank for liquid supply
   Part No. 316 3/8 B501-0256-00-E

7. Denon Model POA-2400 Stereo Solid State Amplifier
   Denon America, Inc., 222 New Road, Parsippany NJ 07054
   Telephone 201-575-7810
   This componet is available at Stereo Stores nationwide

8. Techni-Tool, 5 Apollo Road, Box 36
   Plymouth Meeting PA 19462
   Telephone 215-941-2400
   Distributor for Tech-Dusters, canned Freon-22
   Required for assembling drop generator

9. Freemont Industries, P.O. Box 67, 4400 Valley Industrial Blvd N.
   Shakopee MN 55379-9990
   Telephone 612-445-4121
   Mfg. of "Free-Off-550-Stripper," Strong nozzle cleaner
   and epoxy stripper

10. QuadTech Corporation, formerly GenRad Corporation
    45 Main Street, Boston MA 01740-1107
    Telephone 508-779-8300
    Mfg. of 1539-A Stroboslave, PN 1539-9701

11. MIL Electronics, Inc.
    1 Mill Street, Dracut MA 01826
    Telephone 617-453-8000
    Mfg. of Charge Voltage Module MIL-VH20

12. Orion Industries
    1 Palmer Drive, Suite 202, Londonderry NH 03053
    Telephone 603-43[illegible]4446
    Distributor of Charge Voltage Module MIL-VH20

13. Dow Chemical USA, 2020 Willard H. Dow Center
    Midland MI 48674
    Telephone 800-232-2436
    Manufacturer of Dowicil Preservative used in test fluid

14. Givaudan Corporation, 125 Delawanna Avenue
    Clifton NJ 07014
    Telephone 201-365-8000
    Manufacturer of Giv-Gard preservative used in test fluid

15. 3M Center, Adhesives Systems Division, Building 220-8E
    St. Paul MN 55144-1000
    Telephone 612-733-1110
    1838 B/A Epoxy used for mounting nozzle plates

16. Diagnostic Instruments, Inc., 6510 Burroughs
    Sterling Heights MI 48078
    Telephone 313-731-6000
    Manufacturer of mount for Zeiss microscope

17. Corning Glass Works, Fotoform Products Group
    Corning NY 14831
    Telephone 607-974-4304
    Manufacturer of Fotoceram nozzle plates

18. Leed Plastics Corporation
    781-793 East Pico Boulevard
    Los Angeles CA 90021
    Telephone 213-746-5984
    Distributor of Corning Macor
    Macor is a machinable ceramic made by Corning Glass Co.

19. Aamotron, 3121 East LaPalma, Unit 1
    Anaheim CA 92806
    Telephone 714-630-0110, Fax 714-630-0930
    Driller of small nozzles in Corning Macor Ceramic

20. Advanced Technology Co., David Velazquez
    2858 E. Walnut Street
    Pasadena CA 91107
    Telephone 818-449-2696, Fax 818-793-9442
    Laser drilling, electron beam welding

21. The Microgroup, Inc., 7 Industrial Park Road
    Medway MA 02053
    Telephone 800-255-8823
    Distributor of tubing and fittings
    Laser drilling of small nozzles

22. Mikros Manufacturing, Inc., Dr. Javier Valenzuela
    10 Technology Drive, Unit 2B
    Lebanon NH 03784
    Telephone 603-643-3800, Fax 603-643-4657
    EDM of precise small holes, diffusion welding

23. Costar Nuclepore Corporation
    7035 Commerce Circle, Pleasanton CA 94566
    Telephone 415-463-2530, 800-882-7711
    Manufacturer of membrane filters

24. Gelman Sciences Inc., 600 South Wagner Road
    Ann Arbor MI 48106
    Telephone 313-665-0651, Fax 313-761-1208
    Manufacturer of cartridge filters and housings

25. EDO Corporation, Electro-Ceramic Division
    2645 South 300 West
    Salt Lake City UT 84115
    Telephone 801-486-7481, Fax 801-486-1447
    Manufacturer of piezoelectric elements

26. Morgan Matroc Inc.
    232 Forbes Road, Bedford OH 44146
    Telephone 216-232-8600, Fax 216-232-8731
    Manufacturer of piezoelectric elements

27. Frank E. Fryer, Inc., 650 Northland Boulevard
    Cincinnati OH 45240
    Telephone 513-851-2992
    Distributor of microscopes, television and photographic cameras

28. Ketco Incorporated, 1348 Research Park Drive
    Dayton OH 45432
    Telephone 513-426-9331
    Model shop, composite prototypes, full-size jet engine models

U.S. GOVERNMENT PRINTING OFFICE 750-113